DIFFUSION TENSOR IMAGING IN ACUTE ISCHEMIC STROKE: THE ROLE OF ANISOTROPY IN DETERMINING THE TIME OF ONSET AND PREDICTING LONG-TERM MOTOR OUTCOME

Josep Puig Alcantara

UNIVERSITAT DE GIRONA

Doctoral THESIS

Diffusion tensor imaging in acute ischemic stroke: the role of anisotropy in determining the time of onset and predicting long-term motor outcome

Author:

JOSEP PUIG ALCANTARA

2014

UNIVERSITAT DE GIRONA

Doctoral THESIS

Diffusion tensor imaging in acute ischemic stroke: the role of anisotropy in determining the time of onset and predicting long-term motor outcome

Author:

JOSEP PUIG ALCANTARA

2014

Programa de Doctorat en Ciències Experimentals i Sostenibilitat

Advisors:

Dr. Mar Castellanos
Dr. Joaquín Serena
Dr. Josep Daunis-i-Estadella

Report submitted for the PhD degree at the University of Girona

To my parents and grandparents, for teaching me the value of unpretentious sacrifice as they worked the land. I will always be grateful for everything they have done to enable me to develop my talent. The way I see my work is fruit of my family background.

To my family, Isabel, Pol, and Jan, for all the time my work and commitment to research has stolen from them and for their patience and support. Our children are the driving force in our lives; they make our lives meaningful and bring us great joy.

To Salvador Pedraza, for helping me to realize my ambitions as a researcher and providing me with so many opportunities. I have been fortunate in having you there throughout my career. And to Gerard Blasco, for supporting me day in and day out. Without your help and companionship, my work could never have been so good. To Pepus, for his friendship, trust, and good work. All three of you have been and continue to be fundamental in the success of our work.

To John Giba, for his dependability and professionalism. Our work could never have reached so far from home without your skill and commitment. I hope we can enjoy your collaboration for many years to come.

To Franciscan priest Francesc Costa, for his guidance and advice in hard times; he has been like a second father.

To Mr. and Mrs. Gras, for their unconditional support and trust. I am sure that you look down from heaven with satisfaction.

To my cousin, Miquel Solà, for being a great role model. You showed me that it is possible to be the best and remain humble.

To Albert Barberà, for his vision of working and bet on us: thank you for your support.

To Imma Boada, Alberto Prats, Ferran Prados and Joan San for sharing their professionalism and expertise with me. Those years were very fruitful.

To Marco Essig for all good scope you have given me; I very much appreciate your trust in me.

To the Directors of this thesis: Mar, Joaquín i Pepus. Thank you for your support and experience, which have helped me reach my goal.

LasT but not least, to All who love me and wish me well: having you near rounds out my happiness.

List of Figures

List of Tables

List of abbreviations

ADC	**Apparent diffusion coefficient**
ANOVA	**One-way analysis of variance**
AUC	**Area under the curve**
BI	**Barthel Index**
CR	**Corona radiate**
CS	**Centrum semiovale**
CST	**Corticospinal tract**
DTI	**Diffusion tensor imaging**
DTT	**Diffusion tensor tractography**
DWI	**Diffusion-weighted imaging**
EPI	**Echo-planar imaging**
FA	**Fractional anisotropy**
FLAIR	**Fluid-attenuated inversion recovery**
GE	**Gradient–echo**
GM	**Gray matter**
ICC	**Intraclass correlation coefficient**
IQR	**Inter quanile Range**
MC	**Motor cortex**
MCA	**Middle cerebral artery**
MD	**Mean diffusivity**
MI	**Motricity Index**
m-NIHSS	**Motor scores of the National Institutes of Health Stroke Scale**
MRI	**Magnetic resonance imaging**
mRS	**Modified Rankin Scale**
NIHSS	**National Institutes of Health Stroke Scale**
PLIC	**Posterior limb of the internal capsule**
PMC	**Primary motor cortex**
PWI	**Perfusion-weighted imaging**
rFA	**Ipsilateral-to-contralateral ratio of fractional anisotropies**
ROI	**Regions of interest**
SD	**Standard deviation**
SENSE	**Sensitivity-encoding**
SI	**Signal intensity**
TR/TE	**Repetition time/echo time**
WD	**Wallerian degeneration**
WM	**White matter**

Contents

Resum

Introducció: L'infart cerebral és una de les primers causes de morbi-mortalitat a la nostra societat. La fibrinolisi intravenosa amb activador tissular del plasminogen és el tractament d'elecció durant les primeres 4.5 hores de l'inici dels símptomes. Aproximadament en un terç dels pacients es desconeix el temps d'evolució, pel que el tractament estaria contraindicat. Existeix un gran interés en trobar paràmetres fiables que discriminin el temps d'evolució d'un infart cerebral. El tensor de difusió (DTI, de l'anglès *diffusion tensor imaging*) per ressonància magnètica (RM) és un nou mètode no invassiu que permet estudiar la difusivitat de les molècules d'aigua en els teixits. La DTI aporta informació sobre el grau i direccionalitat de la difusivitat de l'aigua, expresat per la anisotropia fraccional (FA, *fraccional anisotropy*). Actualment, no hi ha evidència científica suficient que sostigui que els índexs anisotròpics juguen un paper important en la determinació del temps d'evolució d'un infart cerebral. D'altra banda, estudis recents han demostrat que l'afectació del tracto corticoespinal (TCE), una de les vies motores principals que regula el moviment voluntari de braços i cames, s'associa a mala evolució motora. Una predicció precoç i precissa del deficit motor contribuïria a un millor maneig dels pacients. Els índexs anisotròpics podrien ser biomarcadors subrrogats de deficit motor a llarg plaç. **Objectius**: els objectius primaris d'aquesta tesi són: (1) valorar els índexs anisotròpics en el parènquima cerebral afectat per l'infart i determinar el potencial predictiu per a discriminar el temps d'evolució d'un infart cerebral; (2) avaluar si l'anisotropia del TCE es correlaciona amb el deficit motor a llarg plaç després d'un infart cerebral. **Material i Mètodes**: S'avaluaren 60 pacients consecutius amb infart a territori de l'artèria cerebral mitja amb un temps inferior a 12 hores d'evolució des de l'inici dels símptomes. El dèficit motor es valorarà mitjançant els subíndexs motors (5a, 5b, 6a, 6b) de l'escala National Institutes of Health Stroke Scale (m-NIHSS) a l'ingrés, dia 3, 30, 90 i als dos anys de l'ictus. La severitat del dèficit motor es va categoritzar en tres graus: grau I (m-NIHSS total de 0), grau II (1–4) i grau III (5–8). El dèficit motor als 2 anys de l'evolució es va valorar mitjançant l'escala d'Índex de Motricitat. Tots els estudis de RM es realitzaren en un equip de 1.5 T. La seqüència de DTI es va

adquirir en 15 direccions. **<u>Resultats</u>**: La rFA al TCE (p=0.001), ratio de diffusivitat mitja cortical (p=0.036), qüoficient aparent de difusió cortical (p=0.009), rT2 al TCE (p=0.006) i hiperintensitat en FLAIR (p<0.001) permeteren discriminar els infarts amb un temps d'evolució inferior o bé superior a 4.5 hores. La rFA al TCE fou el paràmetre més fiable per a discriminar el temps d'evolució d'un infart cerebral en els models de regressió logística binària. Els valors de rFA al TCE superiors a 0.970 mostraren una sensibilitat, especificitat i valors predictius positiu i negatiu de 93.8%, 84.6%, 88.2% i 91.7% per a detectar un infart de menys de 4.5 hores d'evolució, respectivament. D'altra banda, valors baixos de rFA al TCE es correlacionaren amb dèficit motor als 30 dies de l'inici de l'ictus (p<0.001; r = - 0.801). Les variables prectidores independents de dèficit motor a llarg plaç foren la rFA al dia 30, volum d'infart al dia 3, dèficit motor al dia 3 i 30, així com afectació del braç posterior de la capsula interna a l'ingrés. La rFA al dia 30 fou el millor predictor de dèficit motor a llarg plaç (odds ratio 35.45; interval de confiança 95%, 32.23-39.87; p<0.001). Els millors punts de tall de rFA al TCE per tal de discriminar una evolució funcional motora favorable vs. intermitja i intermitja vs. desfavorable als dos anys des de l'inici de l'ictus foren 0.978 i 0.685, respectivament (0.99 àrea sota la corba, p<0.001). **<u>Conclusions</u>**: La quantificació de la rFA al TCE afectat per l'infart podria ser un marcador subrrogat útil de temps d'evolució de l'infart cerebral. El dany axonal a nivell del TCE avaluat per DTI al dia 30 és un factor predictor independent de dèficit funcional motor a llarg plaç en pacients amb infart cerebral.

Resumen

Introducción: El infarto cerebral és una de las primeras causas de morbi-mortalidad en nuestra sociedad. La fibrinolisis intravenosa con activador tisular del plasminógeno es el tratamiento de elección en las primeras 4.5 horas del inicio de los síntomas. Aproximadamente en un tercio de los pacientes se desconoce el tiempo de evolución, por lo que la fibrinolisis estaría contraindicada. Existe un gran interés en detectar parámetros fiables para discriminar el tiempo de evolución de un infarto cerebral. El tensor de difusión (DTI, del inglés *diffusion tensor imaging*) por resonancia magnética (RM) es un nuevo método no invasive que permite estudiar la difusividad de las moléculas de agua en los tejidos. La DTI aporta información sobre el grado y direccionalidad de la difusividad del agua, expresada por la anisotropía fraccional (FA, *fraccional anisotropy*). Actualmente, no existe suficiente evidencia científica que sostenga que los índice anisotrópicos son importantes para determinar el tiempo de evolución de un infarto cerebral. Por otro lado, recientemente se ha demostrado que la afectación del tracto corticoespinal (TCE), una de las vías motoras principales que regula el movimiento voluntario de brazos y piernas, se asocia a mala evolución motora. Una predicción precoz y precisa del déficit motor contribuiría a un mejor manejo de los pacientes. Los índices anisotrópicos podrían ser biomarcadores subrogados de deficit motor a largo plazo. **Objectivos**: Los objetivos primarios de esta tesis son: (1) valorar los índices anisotrópicos en el parénquima cerebral afectado por el infarto y determinar el potencial predictivo para discriminar el tiempo de evolución de un infarto cerebral; (2) evaluar si la anisotropía del TCE se correlaciona con el deficit motor a largo plazo tras un infarto cerebral. **Material y Métodos**: Se evaluaron 60 pacientes consecutivos con infarto en territorio de la arteria cerebral media de menos de 12 horas de evolución. El déficit motor se valorará mediante los subíndices motores (5a, 5b, 6a, 6b) de la escala National Institutes of Health Stroke Scale (m-NIHSS) al ingreso, día 3, 30, 90 y los dos años tras el ictus. La severidad del déficit motor se categorizó en tres grados: grado I (m-NIHSS total de 0), grado II (1-4) y grado III (5-8). El déficit motor a los 2 años de la evolución se valoró mediante la escala de Índice de Motricidad. Todos los estudios de RM se realizaron en un equipo de

1.5 T. La secuencia de DTI se adquirió en 15 direcciones. **Resultados**: La rFA en el TCE (p=0.001), ratio de diffusivitat media cortical (p=0.036) , coeficiente aparente de difusión cortical (p=0.009), ratio de señal T2 en el TCE (p=0.006) e hiperintensidad en FLAIR (p<0.001) permitieron discriminar los infartos con un tiempo de evolución inferior o superior a 4.5 horas . La rFA al TCE fue el parámetro más fiable para discriminar el tiempo de evolución de un infarto cerebral en los modelos de regresión logística binaria. Los valores de rFA en el TCE superiores a 0.970 mostraron una sensibilidad, especificidad y valores predictivos positivo y negativo de 93.8%, 84.6%, 88.2% y 91.7% para detectar un infarto de menos de 4.5 horas de evolución respectivamente. Por otra parte, valores bajos de rFA en el TCE se correlacionó con déficit motor a los 30 días del inicio del ictus (p<0.001; r =-0,801) . Las variables prectidoras independientes de déficit motor a largo plazo fueron la rFA el día 30, volumen de infarto al día 3 , déficit motor al día 3 y 30 , así como afectación del brazo posterior de la cápsula interna al ingreso. La rFA el día 30 fue el mejor predictor de déficit motor a largo plazo (odds ratio 35.45; intervalo de confianza 95% , 32.23-39.87, p<0.001). Los mejores puntos de corte de rFA en el TCE para discriminar una evolución funcional motora favorable vs. intermedia e intermedia vs. desfavorable a los dos años desde el inicio del ictus fueron 0.978 y 0.685 , respectivamente (0.99 área bajo la curva, p<0.001) .

Conclusiones : La cuantificación de la rFA en el TCE afectado por el infarto podría ser un marcador subrogado útil de tiempo de evolución. El daño axonal en el TCE evaluado por DTI en el día 30 es un factor predictor independiente de déficit funcional motor a largo plazo en pacientes con infarto cerebral.

Abstract

Introduction: Stoke is a leading cause of death and disability. Intravenous administration of tissue plasminogen activator is conducted in patients with acute ischemic stoke (AIS) within 4.5 hours of onset. However, around a third of AIS patients do not have accurate onset time and most could not satisfy the inclusion criteria for thrombolysis. Therefore, it is recommended to investigate a reliable method that can determine the onset time of stroke. Magnetic resonance imaging (MRI) using diffusion weighted imaging (DWI) and perfusion-weighted imaging (PWI) is an effective method of identifying good candidates for thrombolysis. Diffusion tensor imaging (DTI) is a recently MRI method which allows the mapping of the diffusion process of molecules, mainly water, in biological tissues, in vivo and non-invasively. Molecular diffusion in tissues is not free, reflecting interactions of molecules with many obstacles, such as fibers and membranes. Therefore, DTI provides information on the predominant direction and degree of tissue water diffusion, commonly expressed as the fractional anisotropy (FA). Diffusion anisotropy MRI detects microstructural changes from ischemic injury, but its real clinical value remains unclear. On the other hand, the corticospinal tract (CST) is the most important motor pathway and motor deficit is one of the most common sequelae of AIS. Early prediction of motor outcome is of interest in stroke management because it contributes significantly to patients' ability to live independently: over 50% of AIS patients have residual motor deficits. More accurate prediction of motor function would enable clinicians and patients to set realistic goals and allocate resources efficiently. DTI-metrics could potentially be used as imaging surrogate markers for long-term motor deficit. **Objectives**: In this thesis the primary objectives are whether (1) to investigate temporal changes of diffusion anisotropy on MRI by analyzing distinct ischemic regions and to test the predictive ability of DTI-metrics to determine time from symptom onset in AIS. The other main objectives are (2) to develop a model to predict which variables in the first month after stroke are more accurate in predicting long-term (2 years) motor outcome. **Material and Methods**: We evaluated 60 consecutive patients with MCA AIS onset clearly within 12 hours admitted to our stroke during a 19-month period. National Institutes of

Health Stroke Scale (NIHSS) to assess clinical deficit at admission, at day 3, at day 30, at day 90, and at 2 years from stroke onset. The m-NIHSS subindex (5a, 5b, 6a, 6b) was used to categorize the severity of limb weakness as grade I (total m-NIHSS score of 0), grade II (m-NIHSS, score of 1–4), or grade III (m-NIHSS, score of 5–8). Motricity Index scores were used to categorize the long-term motor outcome at 2-years follow-up. All scans were performed with an 1.5T MR system. DTI was performed by using a single-shot echo-planar imaging sequence with the sensitivity encoding parallel-imaging scheme (15 noncollinear directions). **Results**: We found that variables with significant differences between infarcts ≤4.5 and >4.5 hours were rFA deep white matter (WM) (p=0.001), mean diffusivity ratio (rMD) cortical grey matter (GM) (p=0.036), apparent diffusion coefficient ratio (rADC) cortical GM (p=0.009), rT2 deep WM (p=0.006), and FLAIR (p<0.001). Logistic binary regression models and receiver operating characteristic demonstrated that rFA deep WM was the most reliable parameter to discriminate between infarcts ≤4.5 hours and those >4.5. The sensitivity, specificity, and positive and negative predictive values for infarct ≤4.5 h of onset by rFA deep WM > 0.970 were 93.8%, 84.6%, 88.2%, and 91.7%, respectively. On the other hand, lower rFA values correlated with motor deficit at day 30 (p<0.001; r=-0.801). Independent predictors of long-term motor outcome were rFA at day 30, infarct volume at day 3, motor deficit at day 3, motor deficit at day 30, and PLIC damage on admission. rFA at day 30 was the best predictor of long-term motor outcome (OR 35.45; 95%CI, 32.23-39.87; p<0.001). The best rFA cutoffs for discriminating good vs. intermediate and intermediate vs. poor outcome at 2 years were 0.978 and 0.685, respectively (AUC=0.99, p<0.001). **Conclusions**: DTI metrics, especially rFA deep WM, may be a surrogate marker of stroke age.Axonal damage in the CST revealed by DTI at day 30 is an independent predictor of long-term motor outcome after stroke.

1. Outline

1.1. Determining of ischemic stroke onset and its relevance

Knowing the onset of acute stroke is a prerequisite for intravenous tissue plasminogen activator, because this treatment is approved by national and international guidelines only within the first 4.5 hours.[1,2] Tissue plasminogen activator is a serine protease found on endothelial cells involved in the breakdown of blood clots. As an enzyme, it catalyzes the conversion of plasminogen to plasmin, the major enzyme responsible for clot breakdown. However, as many as 25% to 30% of patients discover stroke on waking up or have no knowledge of stroke onset, and most could satisfy the inclusion criteria for thrombolysis if the onset were known.[3-5] Therefore, there is an interest for investigating a method that can determine the onset time of stroke.

Magnetic resonance imaging (MRI) is an important tool for detecting ischemic lesions in the hyperacute phase, so diffusion-weighted imaging (DWI) is highly sensitive to ischemic lesions even in the hyperacute period (Figure 1). The intensity of each image element (voxel) on DWI reflects the best estimate of the rate of water diffusion at that specific area. Because the mobility of water is driven by thermal agitation and highly dependent on its cellular environment, the hypothesis behind DWI is that findings may indicate early pathologic change.

Although DWI occasionally fails to detect signal changes in ischemic lesions,[6] it is useful for detecting acute stroke within 3 h of onset. Recent studies reported that the detection rate of DWI was about 80% in acute ischemic stroke patients within 3 h of onset.[7] The problem is, however, that DWI also remains positive long after onset, when patients are no longer in the therapeutic window; therefore, cannot provide information about the time from onset. Nevertheless, DWI and perfusion-weighted imaging (PWI) are effective methods of identifying good candidates for thrombolysis because they enable us to identify areas of ischemic penumbra (DWI-PWI mismatch) as therapeutic targets.[8] On the other hand, fluid-attenuated inversion recovery (FLAIR) imaging has been proposed as a reliable MRI surrogate marker of lesion age, due to its ability to identify patients

within the 4.5-hour therapeutic window with moderate accuracy when the infarct is not hyperintense.[9,10] The pulse sequence on FLAIR is an inversion recovery technique that nulls fluids, and its ability to detect stroke increases gradual with time from onset.
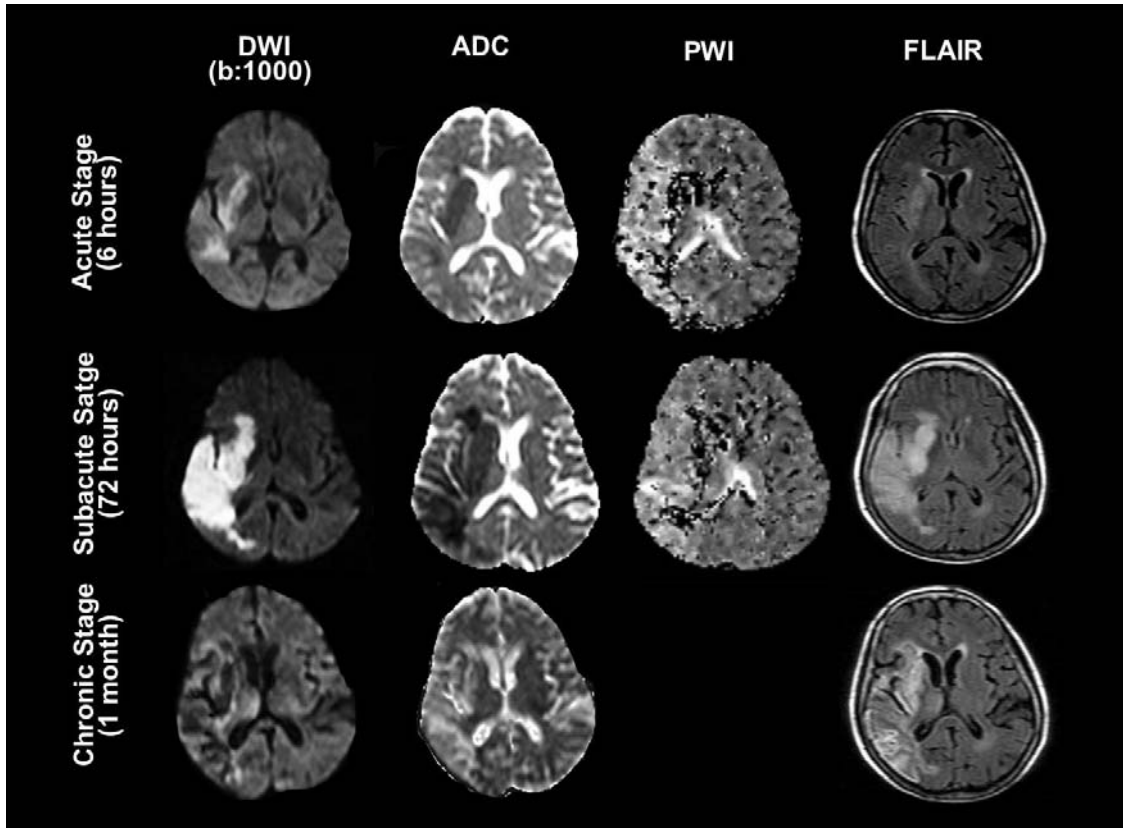
Figure 1. MRI protocol. A 67-year old man with acute right-sided striatocapsular and peripheral middle cerebral artery infaction (seen on DWI images at 6 hours after clinical onset). Perfusion maps reflect hipoperfusion on large area of superficial peripheral territory. Slightly increased signal intensity is shown on FLAIR at 6 hours and markedly increased at 72 hours. A DWI-FLAIR mismatch in acute phase is demonstrated in this case. The infarct volume increased at 72 hours leading to large lesion on deep and peripheral middle cerebral artery territories. Note: The standard MR imaging protocol in acute stroke also includes other sequences, such as T2 gradient echo and angiography (not seen in this figure) in order to exclude cerebral hemorrhage and vascular occlusion, respectively.

Recently, DWI-FLAIR mismatch (ischemic lesion without hyperintensity on FLAIR) has been proposed to identify patients within the therapeutic window of 4.5 h from symptom onset with high specificity and high positive predictive value, lending support to the use of DWI-FLAIR

mismatch as a surrogate marker to identify patients who are eligible for intravenous thrombolysis.[9] Nevertheless, the sensitivity of DWI-FLAIR mismatch to identify patients within 4.5 hours of symptom onset is moderately low (hyperintensity on FLAIR despite short time since stroke onset). Note in this regard that Thomalla et al. have reported that DWI-FLAIR mismatch identify patients within 4.5 h of symptom onset with 62% (95% confidence interval 57-67) sensitivity, 78% (72-84) specificity, 83% (79-88) positive predictive value, and 54% (48-60) negative predictive value;[9] so there is a need for studies focused on identifying others useful imaging parameters.[7,10]

In recent years, much interest has focused on the potential of diffusion tensor imaging (DTI), a relatively novel MRI technique, for in vivo quantification of microstructural damage to cerebral white matter following stroke.[11] In fact, with the advent of DTI, a new era in the study of brain anatomy has started. Classical medical imaging techniques, such as conventional MRI or functional-MRI are not capable of reproducing tract information and only can provide tissue information. DTI is an MRI technique capable of capturing the displacements of particles that are subject to Brownian motion within brain tissues. These displacements give us information about the structural organization and orientation of white matter fibers and, through the technique of tractography, the trajectories of cerebral white matter tracts can be obtained. The anatomical information provided by DTI is oversimplified compared to the underlying neuroanatomy. However, this technique is an important tool to view anatomical structures since it allows in vivo identification of white matter regions, and, should provide new insights into white matter integrity, fiber connectivity, and patient prognosis.

DTI provides information on the predominant direction and degree of tissue water diffusion.[12,13] In the white matter, water diffuses quickly lengthwise along the fibers and slowly perpendicular to fibers, resulting in anisotropic diffusion.[14,15] The degree of anisotropy depends on the level of organization and integrity of the white matter tract and on the degree of freedom of

water diffusion movements by oriented axonal membranes and myelin sheaths. However, although DTI-metrics, such as fractional anisotropy (FA), detect microstructural changes attributable to ischemia, their clinical value as a biological tissue clock remains unclear. [11,16-21] In this research, we aimed to assess the utility of DTI-metrics for distinguishing whether ischemic strokes' age lies within the therapeutic window of less than 4.5 hours from onset in patients with territorial middle cerebral artery (MCA) stroke.

1.2. Predicting long-term motor outcome after ischemic stroke and its relevance

We also investigated the potential of DTI in the corticospinal tract (CST) to predict motor outcome 2 years after stroke. The CST is the major efferent projection white matter fibers that connect motor cortex to the brain stem and spinal cord, and thereby serves as the main conduit of information between the higher cortical structures and the voluntary musculature of the arms, legs, and torso. Most particularly, the fibers of the CST converge into the corona radiate and continue through the posterior limb of the internal capsule (PLIC) to the cerebral peduncle on their way to the lateral funiculus. The CST is the most important motor pathway; motor deficit is one of the most common sequelae of stroke, and its severity correlates with functional disability and reduced quality of life.[22] The accurate prediction of motor deficit is important for management and rehabilitation.[23] Clinical variables such as age, infarct volume, and initial stroke severity measured with a neurologic deficit scale such as the National Institutes of Health Stroke Scale (NIHSS) (Annex 11.1) have consistently been associated with functional outcome after stroke.[24-26]

Neuroimaging studies suggest CST integrity is important for motor outcome.[27-34] DTI assesses the microstructural status of white matter objectively and quantitatively.[35,36] Cross-sectional studies have established DTI regional FA values as surrogate markers of motor deficit after stroke: lower values in affected CST correlate with worse motor function.[34, 37-42] Wallerian degeneration WD consists of the anterograde degeneration of axons and their myelin sheaths after

19

proximal axonal or cell body injury from numerous causes, including stroke. Wallerian degeneration has been demonstrated through animal models, postmortem studies, transcranial magnetic stimulation, and conventional imaging.[43-47] In this respect, we recently demonstrated significant correlations between DTI-measured wallerian degeneration indexes in the CST and NIHSS-measured scores of limb motor deficit (m-NIHSS) 30 days after stroke onset in a relatively large cohort of patients with territorial MCA infarction.[34] Interestingly, decreased anisotropy distal to the infarct on the affected side of the CST, expressed as FA values measured at the rostral pons, correlated significantly with limb motor deficit at day 30.

Acute stroke damage to specific CST regions evident at diffusion tensor tractography (DTT) can predict limb motor outcome.[27-32,48] We recently found that the involvement of the PLIC alone or in combination with other specific CST regions in the first 12 hours after stroke was strongly associated with severe motor deficits in the first 12 hours and with poor motor functional outcome at day 90.[48] The internal capsule is a large and compact fiber bundle that serves as a major conduit of fibers to and from the cerebral cortex and is readily identified on directional DTI color maps. The anterior limb lies between the head of the caudate and the rostral aspect of the lentiform nucleus, while the posterior limb lies between the thalamus and the posterior aspect of the lentiform nucleus. The anterior limb passes projection fibers to and from the thalamus (thalamocortical projections) as well as frontopontine tracts, all of which are primarily anteroposteriorly oriented in contradistinction to the posterior limb, which passes the superior-inferiorly oriented fibers of the corticospinal, corticobulbar, and corticopontine tracts. This gives the anterior and posterior limbs distinctly different colors on directional DTI maps. Although damage to the centrum semiovale and corona radiata at day 3 was also associated with poor motor outcome at day 90, PLIC damage in the first 12 hours after stroke was clearly the best predictor of motor deficits and of their severity. To our knowledge, no prospective studies have assessed DTI's ability to predict long-term motor

outcome after stroke. We assessed whether FA values and stroke location on DTT of the CST can predict motor outcome 2 years after stroke.

Thus far, our main contributions to clinical DTI research on stroke lend support to the idea that motor outcome is highly dependent on lesion location and the extent to which acute stroke affects the CST.[34, 48] In particular, PLIC damage could be considered an early imaging predictor of poor motor outcome.[48] These findings have implications for the use of lesion mapping techniques in the prognosis of motor outcome after stroke and for establishing more effective criteria for enrolling and evaluating patients in rehabilitation programs.

2. Background

2.1. Diffusion Tensor Imaging: acquisition process

DTI is an MRI technique that can be used to characterize the orientation properties of the diffusion process of water molecules. Molecular diffusion refers to the random translational motion of molecules (Brownian motion) that result from the thermal energy carried by these molecules.[49] The displacement of the molecules varies according to the features of the analyzed environment. To measure diffusion, the Stejskal-Tanner imaging sequence is used.[50] This sequence uses two strong gradient pulses, symmetrically positioned around a 180 refocusing pulse, allowing for controlled diffusion weighting (Figure 2).
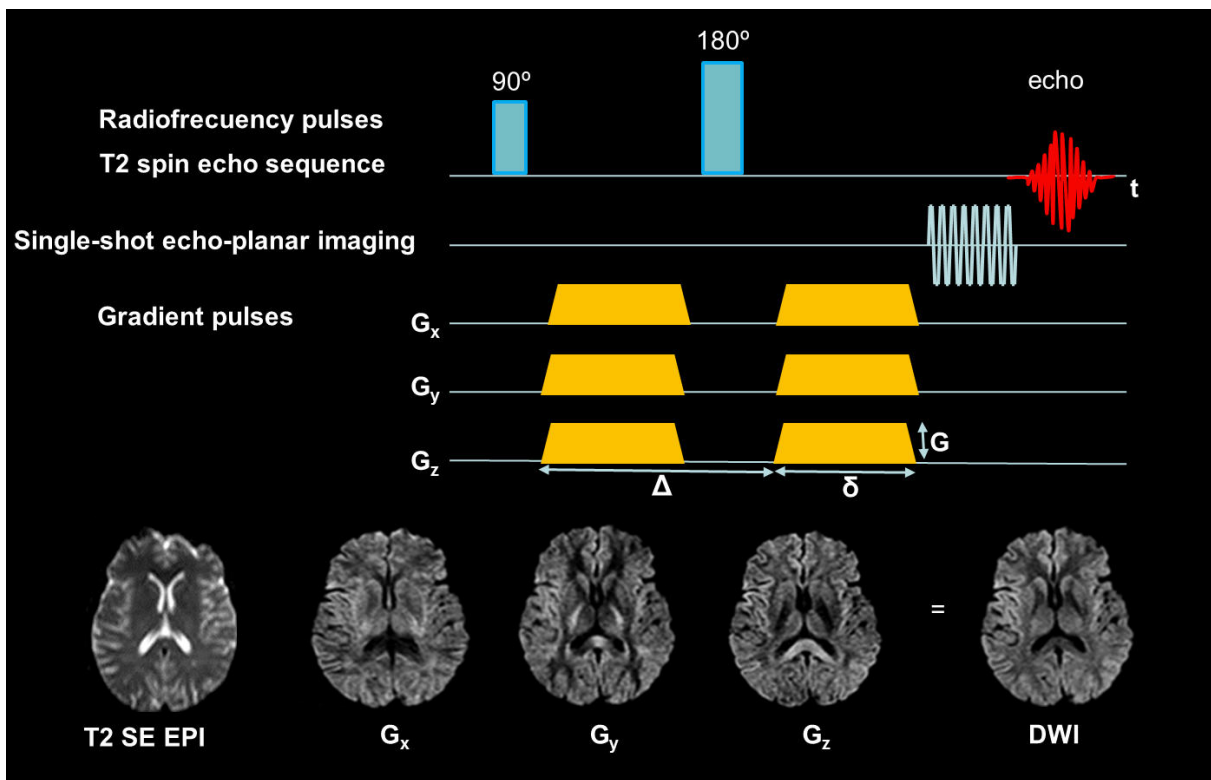
Figure 2. DTI acquisition process. Pulse sequence diagram for a DWI acquisition shows that 3 diffusion-sensitizing gradients are added to a SE sequence, 1 before and 1 after the 180° refocusing pulse. The DW factor b depends on the amplitude of gradient (G), the duration of each gradient (δ), and the interval between the onset of the diffusion gradient before the refocusing pulse and that following the refocusing pulse (Δ).

2.2. Diffusion Tensor Imaging: concept of anisotropy

Basically, two diffusion movements can be found, isotropic and anisotropic (Figure 3). Isotropic movement corresponds to environments without a concentration gradient, where the probability of displacement of molecules is equal in all directions, and the mean molecular displacement and the flux are zero. The random mobility of these molecules is statistically well described by a Brownian movement. Anisotropic movement corresponds to a medium with highly oriented barriers where the tortuosity is different for each direction in the space, leading to an anisotropic diffusion. Water molecules located in fiber tracts are more likely to be anisotropic, since they are restricted in their movement as they move more in the dimension parallel to the fiber tract rather than in the two dimensions orthogonal to it, whereas water molecules dispersed in the rest of the brain have less restricted movement and therefore show more isotropy. Therefore, the underlying physical process of diffusion causes a group of water molecules to move out from a central point and gradually reach the surface of an ellipsoid if the medium is anisotropic (it would be the surface of a sphere for an isotropic medium).[49] The ellipsoid formalism also works as a mathematical method of organizing tensor data. Measurement of an ellipsoid tensor further permits a retrospective analysis to obtain information about the process of diffusion in each voxel of the tissue.[13] DTI is a relatively new MRI technique that makes it possible to map the diffusion of molecules, mainly water, in biological tissues, in vivo and non-invasively.[13] Molecules cannot diffuse freely in normal tissues because they interact with many obstacles, such as fibers and membranes.[15] Once we have measured the voxel from six or more directions and corrected for attenuations due to T2 and T1 effects, we can use information from our calculated ellipsoid tensor to describe what is happening in the voxel.
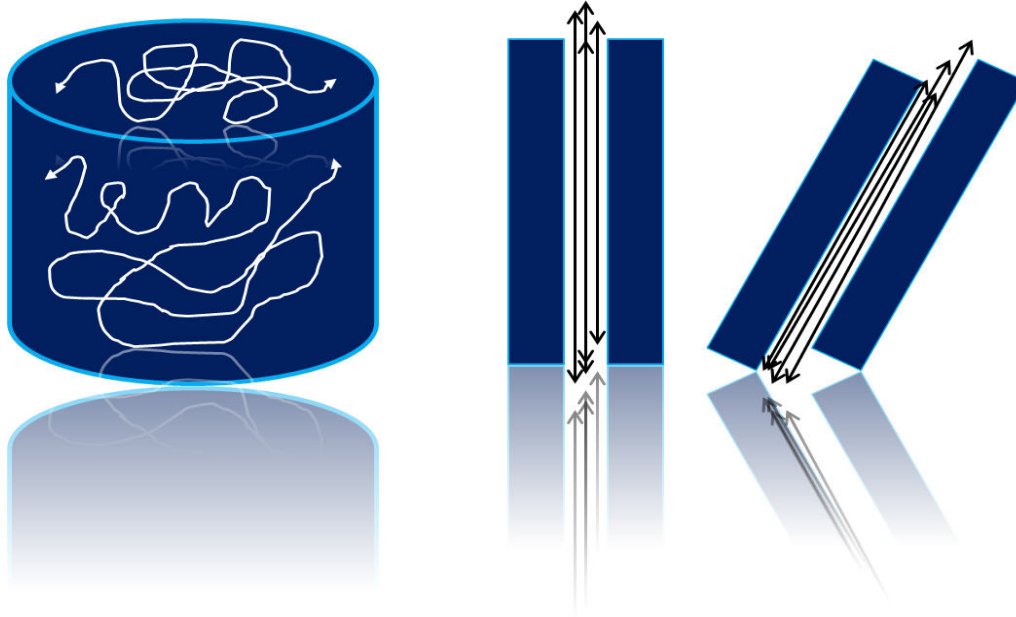
Figure 3. Isotropy and anisotropy. Diffusion movements of a molecule in an isotropic environtment (left) and anisotropic one (right).

2.3. DTI-metrics: eigenvalues, eigenvectors, mean diffusivity and fractional anisotropy

The ellipsoid itself has a principal long axis and then two small axes that describe its width and depth. The three axes are perpendicular to each other and cross at the center point of the ellipsoid. We call the axes in this setting eigenvectors and the measures of their lengths eigenvalues (Figure 4). The lengths are symbolized by letter λ. The long axis pointing along the axon direction will be λ_1 (also called longitudinal diffusivity or axial diffusivity) and the two small axes will have lengths λ_2 and λ_3 (radial diffusivities).[12]

Mean diffusivity is a measure that summarizes the total diffusivity, which is the sum of the three eigenvalues divided by 3; as follows [35]

$$MD = [\lambda_1 + \lambda_2 + \lambda_3] / 3$$

Aside from describing the amount of diffusion, it is often important to describe the relative degree of anisotropy in a voxel of brain tissue. At one extreme would be the sphere of isotropic diffusion and at the other extreme would be a cigar- or pencil-shaped very thin spheroid. The simplest measure is obtained by dividing the longest axis of the ellipsoid by the shortest $= (\lambda_1/\lambda_3)$.

However, this proves to be very susceptible to measurement noise, so increasingly complex measures were developed to capture the measure while minimizing the noise.[12] An important element of these calculations is the sum of squares of the diffusivity differences, as follows [2,12, 35]

$$(\lambda_1 - \lambda_2)^2 + (\lambda_1 - \lambda_3)^2 + (\lambda_2 - \lambda_3)^2$$

We use the square root of the sum of squares to obtain a sort of weighted average— dominated by the largest component. One objective is to keep the number near 0 if the voxel is spherical but near 1 if it is elongate.

This leads us to the fractional anisotropy (FA), which is the square root of the sum of squares of the diffusivity differences, divided by the square root of the sum of squares of the diffusivities.[51]

$$FA = \frac{\sqrt{3}}{\sqrt{2}} \frac{\sqrt{(\lambda_1 - \langle\lambda\rangle)^2 + (\lambda_2 - \langle\lambda\rangle)^2 + (\lambda_3 - \langle\lambda\rangle)^2}}{\sqrt{(\lambda_1)^2 + (\lambda_2)^2 + (\lambda_3)^2}}$$
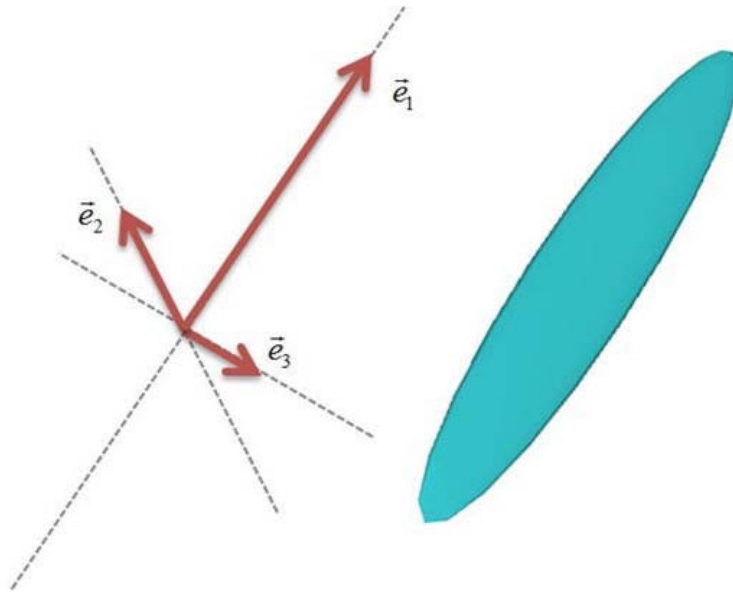
Figure 4. Diagram of diffusion tensors and DTI-metrics. (a) The diffusion tensor is shown as an ellipsoid with its principal axes along the eigenvectors (e_1, e_2, e_3). The principal direction gives a good estimate of the regions where there is only one fiber population, because fibers are aligned along a single axis. The different DTI-metrics that have been proposed are obtained from diffusion tensor eigenvalues or eigenvectors.

Therefore, DTI provides information on the predominant direction and degree of water diffusion in tissues, commonly expressed as fractional anisotropy (FA). In the white matter, water diffuses quickly lengthwise along the fibers and slowly perpendicular to fibers, resulting in anisotropic diffusion.[14,15] The degree of anisotropy depends on the level of organization and integrity of the white matter tract and on the degree of freedom of water diffusion movements by oriented axonal membranes and myelin sheaths.[12,13] DTI enables in vivo visualization and quantification of microstructural damage to white matter tracts (Figure 5).
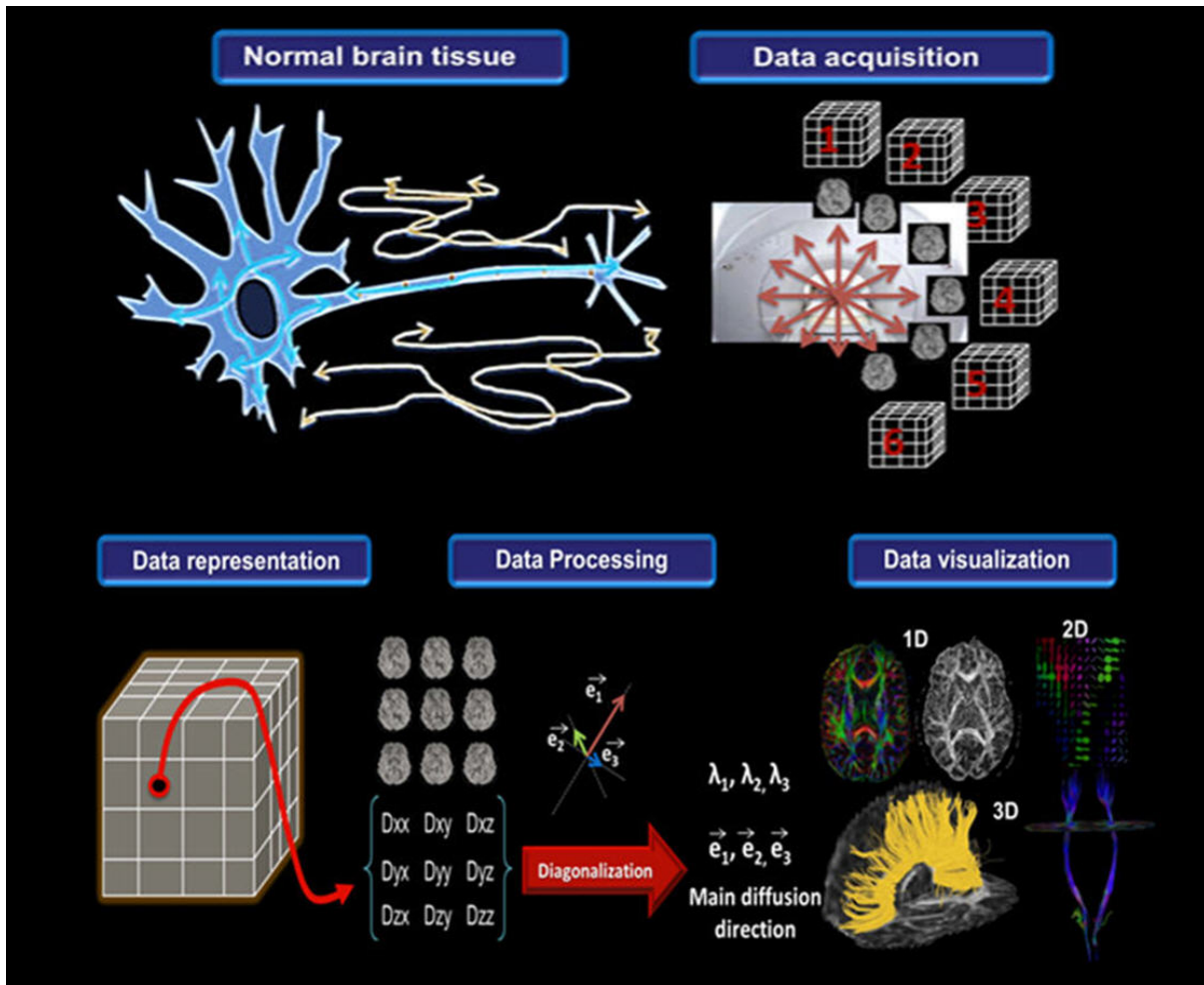
Figure 5. Diffusion tensor imaging: from anisotropic water diffusion to tractography. DTI provides diagnostic information on the microstructural status of brain tissue by quantifying anisotropic indexes that show the predominant direction and degree of water diffusion: water molecules move mostly parallel to the fiber tract with respect to scanner geometry (x, y, z axes) and impose directional dependence (anisotropy) on diffusion measurements. The three-dimensional diffusivity is modeled as an ellipsoid whose orientation is characterized by three eigenvectors (e_1, e_2, e_3) and whose shape is characterized three eigenvalues (λ_1, λ_2, λ_3). This ellipsoid model is fitted to a set of at least six noncollinear diffusion measurements by solving a set of matrix equations involving the diffusivities and requiring a procedure known as matrix diagonalization. The major eigenvector reflects the direction of maximum diffusivity, which, in turn, reflects the orientation of fiber tracts. Therefore, DTI captures information about diffusion in several directions and reduces it to a tensor that describes the local water diffusion at the voxel level. For each voxel the diffusion tensor, from which eigenvalues and eigenvectors are obtained, can be calculated. Processing and visualization techniques facilitate the clinical interpretation.

2.4. DTI visualization data: 1D, 2D and 3D techniques for clinical analysis

Visualization techniques are fundamental for DTI interpretation. Focusing in tensor-based processing techniques, most of the visualization strategies that have been proposed are based on reducing the dimensionality of the data by extracting relevant information from the diffusion tensor. This data can be analyzed by 1D, 2D and 3D visualization strategies.[52] (Figure 6).
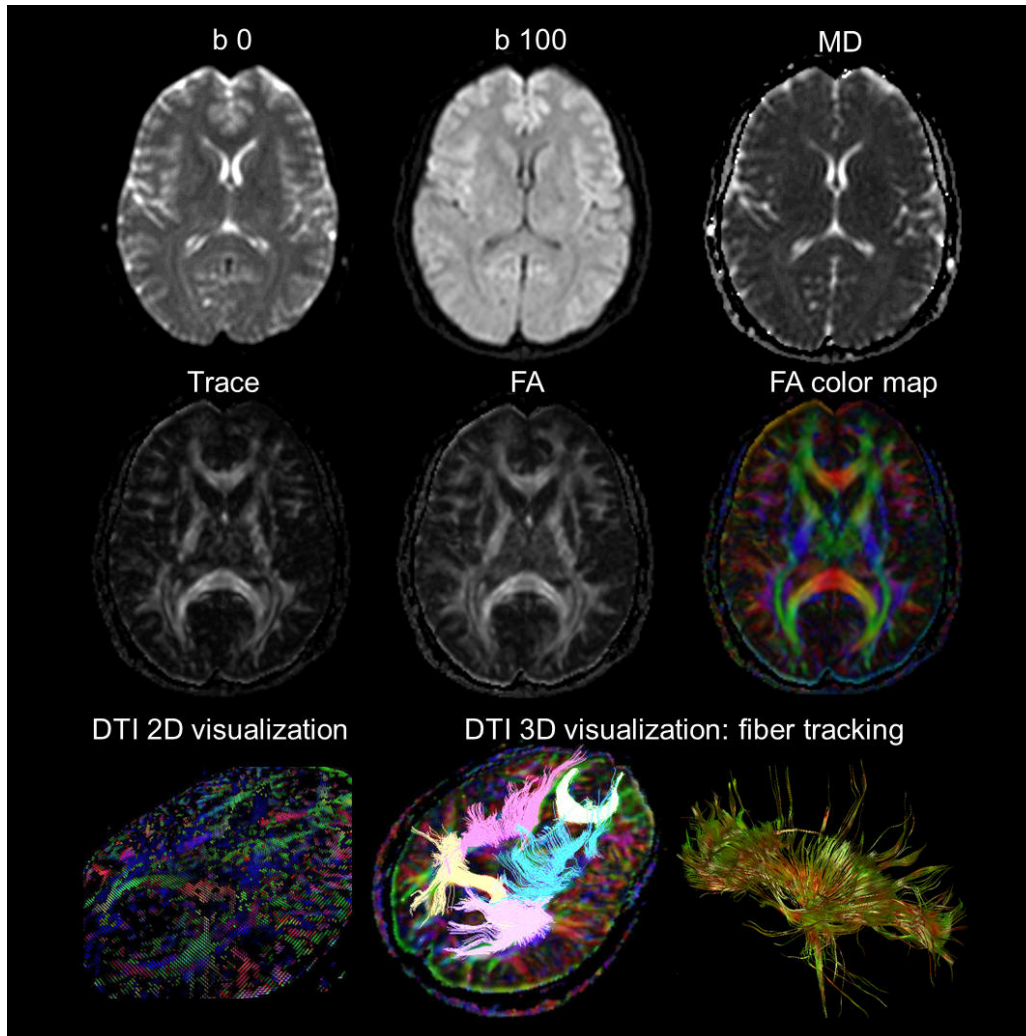
Figure 6. DTI visualization data. 1D anisotropy indices: Grey images are obtained by assigning a grey codification to the anisotropy measure. RGB images assign the fiber color direction: red for left-right fibers, blue for craneocaudal fibers, and green for anterior-posterior fibers. 2D visualizations considering cuboids and ellipsoids as glyphs. Tracking techniques can be applied to generate fiber tracts tridimensionally.

1D visualization techniques generate 2D images from 1D scalar values or indices obtained from tensor within voxels. These scalar values are visualized using a grey or a color scale 2D images. Currently, such an approach is the most used in clinical practice since grey and color coded images are simple and easy to interpret. The different indices that have been proposed are obtained from diffusion tensor eigenvalues or eigenvectors.[53,54]

FA is the most popular DTI-metric used in clinical setting. The main drawback of 1D visualization techniques is the fact that only one part of DTI data is represented in the image and hence important information is lost.

To overcome this limitation, 2D visualization techniques are proposed. These techniques use a graphical representation of eigenvalues (λ_i) and eigenvectors (e_i) to express the degree of diffusion anisotropy present in the tissue of interest. This information can be viewed as an ellipsoid with the length of principal axes described by the tensor eigenvalues and the directions given by the tensor eigenvectors and the length to eigenvalues.[54]

Tensor shapes are described by a combination of linear, planar, and spherical measures, and anisotropic measures are interpreted by considering how much the diffusion ellipsoid deviates from the isotropic case represented as a sphere. 1D and 2D visualization techniques only represent a part of the information obtained from DTI. Moreover, they are not capable of reproducing fiber tracts or generate a comprehensive view of the whole brain model.

To overcome this limitation, 3D visualization techniques have been proposed. These do not consider the information distributed onto a single plane, but the information of the 3D model. The basic approaches reduce the tensor data created from the DTI model to a vector field where the vector direction is given by the maximum eigenvector obtained from the tensor. Then, tracking techniques can be applied to generate paths representing fiber tracts and reproduce in this way white matter fiber maps.

The most popular fiber tracking technique is the streamline approach.[55,56] Streamline algorithms assume that the direction of a fiber is collinear with the maximum diffusivity direction given by the main eigenvector of tensor D. To create the white matter connectivity map, a set of tracking points or seeds are defined. Then, for each seed, a pathway that follows the maximum diffusivity direction is traced until the boundary of the data set is reached or the value of certain measures at the current curve point lies outside a previously specified admissible range of values.

These techniques can be grouped into different categories: deterministic, that follows the major diffusion tensor eigenvector [57,58], non-deterministic, that randomly perturbs the main fiber direction at each location[59], probabilistic, that calculates a spatial probability distribution of connectivity from the seed point [60-62], and finally, global optimization algorithms, that generate the most optimal path between two brain regions by minimizing a cost function that usually describes the smoothness of the path and the goodness of fit of the path configuration to the underlying diffusion signal.[63,64]

In short, diffusion tensor tractography uses data acquired through DTI to reconstruct a 3D macroscopic orientation of the white matter fibers that enables the specific topographic relation between lesion location and CST fibers to be evaluated.[12,13]

2.5. The role of anisotropy in determining the time of onset of stroke

DTI's ability to precisely detect water molecules' diffusivity makes this technique especially interesting as a potential way to evaluate the impact of ischemic stroke on the microarchitecture of the brain. On the one hand, during an ischemic stroke, a lack of oxygen and glucose leads to a breakdown of the sodium-calcium pumps on brain cell membranes, which in turn results in a massive buildup of sodium and calcium intracellularly.

This causes a rapid uptake of water and subsequent swelling of the cells.[65] DTI could make it possible to study early changes in brain parenchyma caused by cytotoxic edema in more detail.[11,17,20] The quantification of anisotropic indices could be used as a biologic clock that would enable the time from acute stroke onset to be determined better.

On the other hand, once tissue damage from cerebral ischemia is established, DTI might provide prognostic information. In this sense, DTT depiction of early involvement of specific white matter tracts, such as the CST, has been recently reported as an indicator of poor functional outcome.[28,32,48]

International guidelines for intravenous thrombolysis exclude patients in whom the time of stroke symptom onset is unknown.[1,2] Intravenous thrombolysis with tissue plasminogen activator is limited to patients with acute ischemic stroke of less than 4.5 hours from stroke onset using unenhanced brain computed tomography.

As many as 25% to 30% of acute stroke patients do not have accurate information about the time of onset; consequently, thrombolysis is precluded in many patients who might benefit from this treatment.[3,5] These circumstances have raised great interest in looking for surrogate markers of lesion age.

Multiparametric MRI has been used to identify patients who are likely to benefit from thrombolysis. Different sequences are sensitive to different aspects of tissue pathophysiology in acute cerebral ischemia (Figure 7).[66]
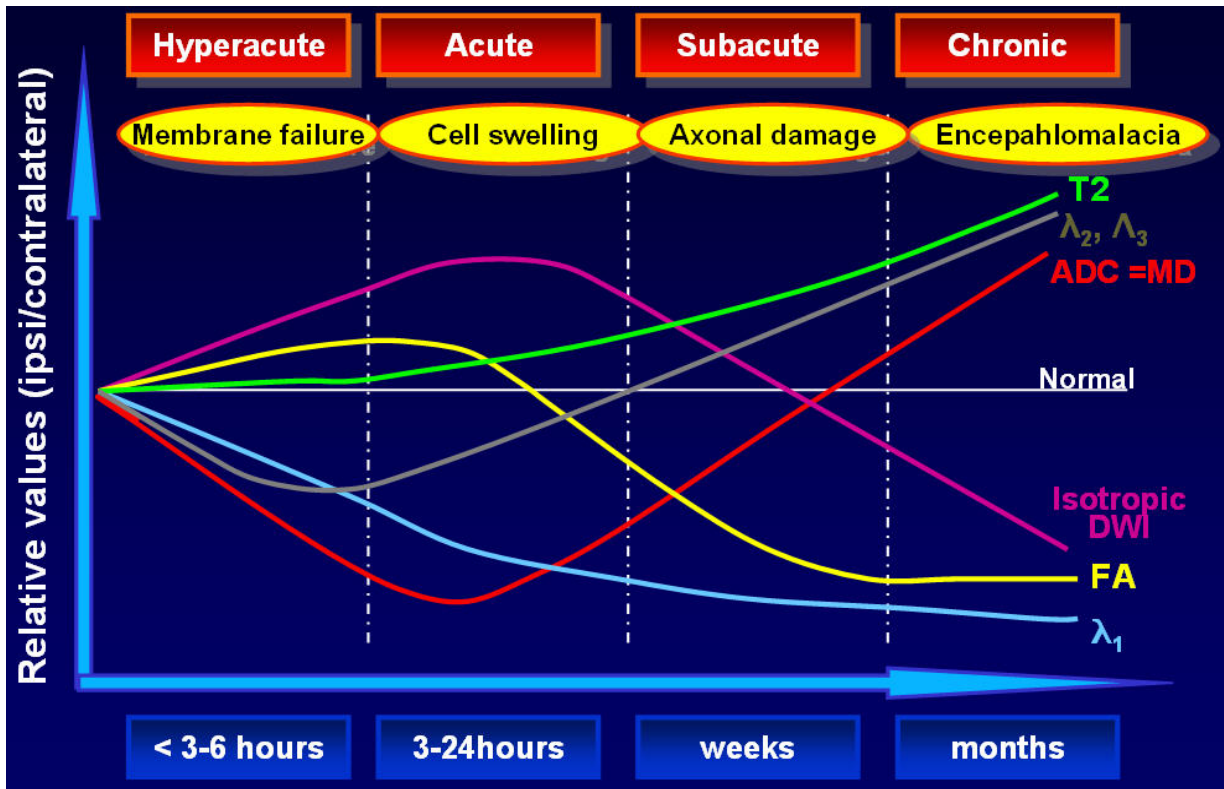
Figure 7. Time course of diffusivity indices in stroke. Four stages were defined based on detectable chronological changes in water molecular diffusivity. At hyperacute phase, a slight increase in fractional anisotropy (FA) occurs, which is known to be caused mainly by reductions in λ_2 and λ_3. At acute phase, these once-reduced transverse eigenvalues begin to increase, probably due to cell swelling. This process cannot be detected directly by observing eigenvalues until one of the transverse eigenvalues exceeds the value of the contralesional side. This point was defined as the start of subacute phase of the infarct lesion. T2 indicates hyperintensity on T2WI; $\lambda 1$, major eigenvalue, longitudinal or axial diffusivity; $\lambda 2$ and $\lambda 3$, minor eigenvalues or radial diffusivities; ADC, apparent diffusion coefficient; MD, mean diffusivity; and DWI, diffusion weighted imaging.

Alterations in water diffusion can be detected with diffusion-weighted imaging (DWI) within 3 min from onset of ischemia, and a net increase in water can be detected as an increase in T2 signal 1 h to 4 h from the onset of ischemia.[66-68] Fluid-attenuated inversion recovery (FLAIR) imaging is a T2-weighted imaging sequence and an integral part of common MRI protocols for stroke.[69] FLAIR is reportedly able to demonstrate signal changes based on the time interval since onset: it is highly sensitive to subacute ischemic lesions, but commonly cannot be used to detect lesions during the first few hours after stroke onset.[10] Recently, research using a large multicenter

dataset showed that DWI-FLAIR mismatch (ischemic lesion without hyperintensity on FLAIR) can identify patients within the therapeutic window of 4.5 h from symptom onset with high specificity and high positive predictive value, lending support to the use of DWI-FLAIR mismatch as a surrogate marker to identify patients with acute stroke who are eligible for intravenous thrombolysis.[9] Nevertheless, the sensitivity of DWI-FLAIR mismatch to identify patients within 4.5 hours of symptom onset was low (hyperintensity on FLAIR despite short time since stroke onset), showing the need for studies based on other imaging parameters.

Diffusion anisotropy detects microstructural changes from ischemic injury, but its role in determining the onset time of stroke remains unclear. Some previous studies found increased FA values in cerebral areas affected by hyperacute stroke.[18,70] Although the cellular basis of this phenomenon remains to be elucidated, it seems that oligodendrocyte swelling from cytotoxic edema could result in extra-axonal water and compression of the axoplasm by swollen myelin sheaths.

This translates to greater decline in radial than axial water diffusivity in infarcted axons, which could explain the increase in rFA values in the first hours after stroke onset. FA values are significantly elevated (up to 25%) only ≤7 hours of symptom onset and then decrease (~15% declines) from 8 h to 34 h after stroke.[19] Comparing anisotropy parameters in the lesion with those of the contralateral side, one study showed elevated FA ratios mainly within 24 hours and reduced rFA mainly after 24 h.[21] Another study showed a reduced rFA in white matter and constant rFA in gray matter.[71] The breakdown of the axons results in massive water accumulation in axons that translates to hyperintensity in FLAIR and T2-weighted images when the infarct evolves over time. Large decreases in FA suggest loss of cellular integrity with irreversible axonal injury not reflected on conventional MRI.[16] Therefore, diffusion anisotropy detects microstructural changes from ischemic injury, but its value as a MRI surrogate marker of lesion age is not clear.

2.6. The role of DTI in predicting motor outcome in stroke patients

As mentioned above, diffusion anisotropy detects microstructural changes from ischemic injury, but its real clinical value remains unclear. The CST is the most important motor pathway and motor deficit is one of the most common sequelae of acute stroke.[22] Early prediction of motor outcome is of interest in stroke management because motor outcome contributes significantly to patients' ability to live independently: over 50% of acute stroke patients have residual motor deficits.[22,23] More accurate prediction of motor function would enable clinicians and patients to set realistic goals and allocate resources efficiently. DTI metrics could potentially be used as imaging surrogate markers for long-term motor deficit.

On the subject of motor outcome after acute ischemic stroke, several observational studies have demonstrated that the grade of initial motor deficit is the most important determinant of motor recovery.[24] Other valid predictors in regression models have included infarct site, volume of stroke, age, demographics, comorbidities, infarct side, and stroke subtype.[24,25] Several neurophysiological and structural imaging studies have provided evidence that motor outcome is heavily dependent on the integrity of the motor fibers.[27,34] Thus, the involvement of motor-related cortical regions, corona radiata, and internal capsule progressively decrease the probability of upper limb functional recovery.[26,48]

Recently, these findings were complemented by DTI studies that demonstrated the usefulness of DTT for predicting poor motor outcome when infarcts involve the CST (Figure 8).[27-34] In this respect, recently have been demonstrated that decreases in FA can be interpreted as wallerian degeneration and proposed this finding as an index of axonal damage, so decreased FA values in the damaged CST correlates with motor impairment one month after stroke.[34]
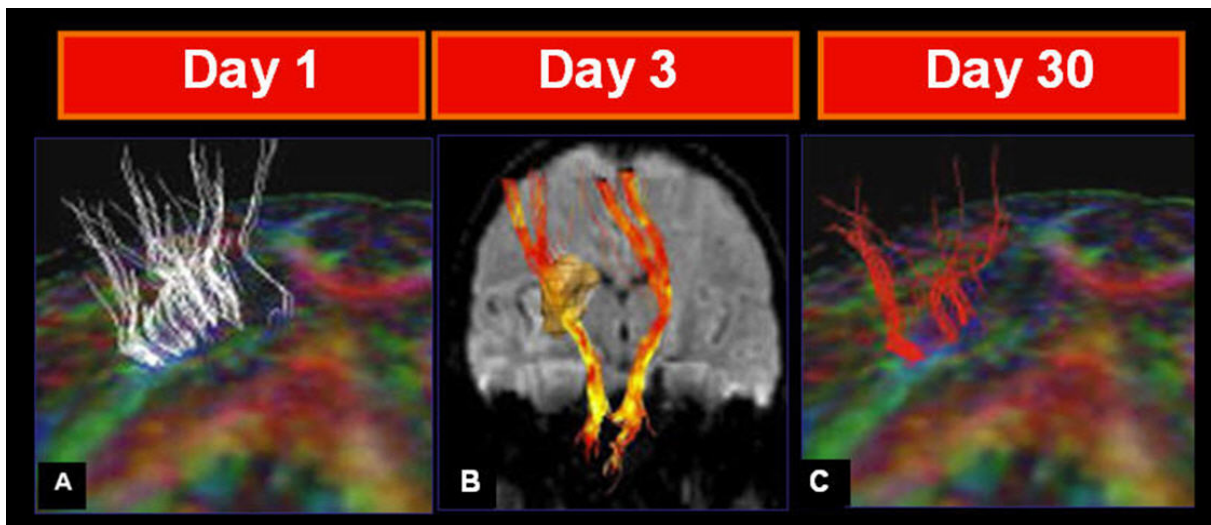
Figure 8. Dynamic changes along the CST after deep territory middle cerebral artery infarction from the patient's admission to 1 month follow-up. Marked axonal loss is shown on tractography at day 30. This case demonstrates that infarct size (B) (8 mL) correlates only modestly with functional outcome (moderate-severe hemiparesis at day 30). This may be largely because volume measures do not take account of variations in lesion location at functional pathways involved. The posterior limb of internal capsule was affected in this patient.

The involvement of the PLIC alone or in combination with other specific CST regions in the first 12 hours after stroke have been found strongly associated with severe motor deficits and poor motor functional outcome at day 90.[48] Despite this evidence, prospective studies have not assessed DTI's ability to predict long-term motor outcome after stroke.

3. Hypothesis and Objectives

The main hypotheses of this thesis are:

- Changes in the anisotropy in the infarct core could detect cerebral infarctions up to 4.5 hours of evolution, so that DTI-metrics might be used as a surrogate marker of stroke age.

- The quantification of microstructural damage to cerebral white matter following stroke (axonal damage) revealed by DTI at month could be an independent predictor of long-term motor outcome.

Owing to the foregoing, the primary objectives of this research will be:

- To test whether DTI-metrics analyzing distinct ischemic regions can be used to determine whether acute stroke patients are within the recommended time window for thrombolysis.

- To assess whether anisotropy using DTI in the CST correlates with long-term motor outcome after MCA acute stroke.

Finally, the secondary objectives of this research will be:

- To develop a model to predict which variables in the first month after stroke are more accurate in predicting long-term (2 years) motor outcome.

- To calculate the best FA cutoff to discriminate long-term motor deficit.

4. Material and Methods

4.1. To test whether changes in the anisotropy in the infarct core could detect infarctions up to 4.5 hours of evolution

4.1.1. Patients

For this purpose, 60 consecutive patients with first-ever middle cerebral artery (MCA) territory infarction within 12 hours of symptom onset were studied.

We excluded patients with cerebral hemorrhage, significant preexisting non-ischemic neurological deficit (including dementia or extrapyramidal disease), or a history of prior stroke that would hinder the interpretation of clinical and radiological data.

The study was approved by the local ethics committee of the Hospital Universitari Dr Josep Trueta and all patients or their relatives provided informed written consent.

4.1.2. Clinical assessment

Patients underwent neurological examination, including National Institutes of Health Stroke Scale (NIHSS) score, by a certified neurologist at admission, without knowledge of the MRI findings. Patients were treated according to published guidelines[1].

4.1.3. MR imaging protocol

All patients underwent MR examination on a 1.5-Tesla scanner (Intera, Philips Medical Systems, Best, the Netherlands) with a sense head coil. The protocol included axial trace diffusion-weighted imaging (DWI), fluid-attenuated inversion recovery (FLAIR), gradient–echo (GE) T2*-weighted, perfusion-weighted imaging, time-of-flight angiography, and DTI sequences.

DTI data were acquired using single-shot echo-planar imaging (EPI) sequences with the sensitivity-encoding (SENSE) parallel-imaging scheme (acceleration factor 2) after contrast agent administration.

DTI with sensitivity encoding helped reduce scan time and minimize the susceptibility and distortion artifacts typically associated with EPI sequences. Diffusion-sensitized gradients were applied along 15 non-collinear directions with a b value of 1000s/mm^2. Diffusion-weighted b0 images were also obtained.

Other acquisition parameters were repetition time/echo time (TR/TE) 6795/72 ms, field of view 23 x 23-cm, and matrix size 112 x 112. Forty-five contiguous 3 mm axial slices covering the entire brain and brainstem were acquired parallel to the anterior-posterior line. DTI scanning time was 3 minutes 10 seconds.

4.1.4. Data processing

DTI data were transferred to an offline workstation for post-processing and visually checked for quality. Diffusion-encoded, FA-weighted images were elaborated using the calculation scheme proposed by Pajevic and Perpaoli.[14] Color FA maps were generated following the standard convention (red, left-right; green, anteroposterior; and blue, superior-inferior).

Diffusion tensor images were coregistered; two expert neuroradiologists (8 and 9 years of experience) used NeuroScape 2.0 MR Stroke Edition (Olea Medical, La Ciotat, France) to place free-hand regions of interest (ROIs) on deep and cortical gray matter (GM), deep white matter (WM) at the level of the corticospinal tract (CST), and subcortical WM in the slice where the infarct had the largest diameters on diffusion-weighted sequences (Figure 9).

They measured FA, mean diffusivity (MD), apparent diffusion coefficient (ADC), and T2-weighted signal intensity (SI) in the ipsilateral affected side and in the homologous contralateral regions, and then calculated the ipsilateral-to-contralateral ratios (r).
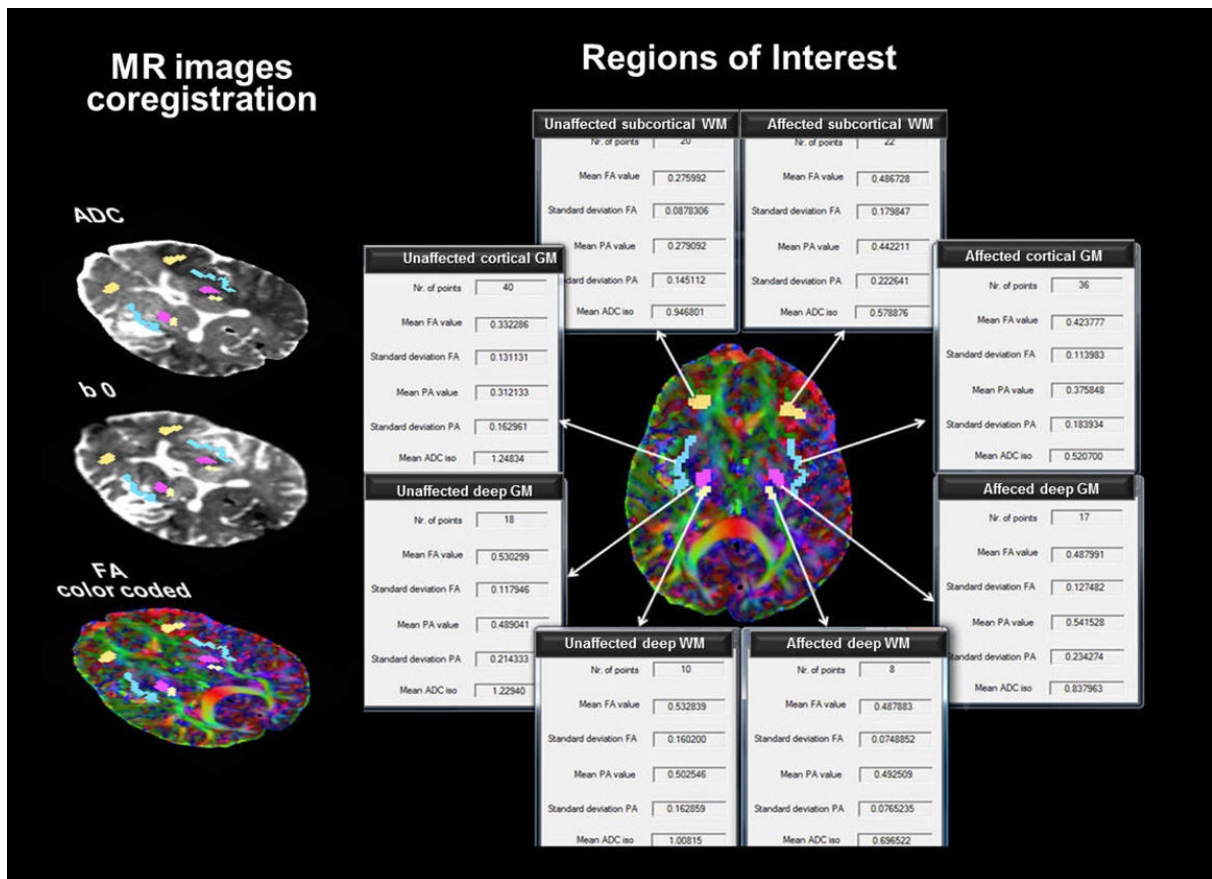
Figure 9. ROIs measurement. DTI-metrics assessment on deep and cortical gray matter, deep white matter at the level of the corticospinal tract, and subcortical white matter affected by acute stroke, as well as in the homologous contralateral regions using ROIs.

Hyperintensity in infarcted tissue was considered FLAIR-positive; discordant FLAIR ratings were resolved by consensus. Interobserver agreements were calculated. The two measurements were averaged for statistical analysis.

4.1.5. Statistical analysis

Data are presented as mean with standard deviation values for each group. The statistical evaluation of the results was based on a one-way analysis of variance (ANOVA) with the

Bonferroni correction. Levene and Bartlett tests were used to test whether the samples had equal variances, and then ANOVA tests were applied to examine the relationship of mean FA values on the affected side of the CST and of rFA with the clinical scores at admission, at day 3, and at day 30.

To compare first and second measurements of the observer number one (intraobserver reliability) and to compare the measurements of two independent observers (interobserver reliability), Kappa statistics was used. The FA values calculated are based on the average of the mean values obtained by two raters. All statistical evaluations were performed using Minitab version 15.1.0.0 (Minitab Inc, State College, Pennsylvania).

4.2. To test whether quantification of microstructural damage to white matter following stroke by DTI at month could be an independent predictor of long-term motor outcome

4.2.1. Patients

For this purpose, 89 consecutive patients with first-ever MCA stroke within 12 hours of onset were scanned; data from 19 patients were incomplete at 2 years due to stroke recurrence (n=6; 6.73%), death (n=9; 10.10%), or motion artifacts (n=4; 4.48%).

Analyses were therefore based on 70 subjects (28 women), with a median of age of 72 years and a standard deviation equal to 12 years.

Patients with cerebral hemorrhage, significant preexisting non-ischemic neurological deficit (including dementia or extrapyramidal disease), or a history of prior stroke that would hinder the interpretation of clinical and radiological data were excluded.

The study was approved by the local ethics committee of the Hospital Universitari Dr Josep Trueta and all patients or their relatives provided informed written consent.

4.2.2. Clinical assessment

Patients underwent neurological examination, including National Institutes of Health Stroke Scale (NIHSS) score, by a certified neurologist at admission. This examination was done also at day 3, and repeated at day 30 after stroke onset.

Based on the motor scores of the NIHSS (5a, 5b, 6a, 6b) (m-NIHSS), severity of limb weakness was categorized into grade I (total m-NIHSS scores of 0), grade II (m-NIHSS:1-4), and grade III (m-NIHSS: 5-8). All m-NIHSS assessments were performed without knowledge of the MRI findings.

Severity of motor deficit at 2 years was categorized by Motricity Index (MI) score into three categories: no deficit (total MI score 100), slight-moderate deficit (MI 99-50), or severe deficit (MI<50).

The modified Rankin Scale (mRS) and Barthel Index (BI) were used to measure disability and dependence in activities of daily living at day 90. Poor overall outcome was defined as mRS>2 and/or BI <60.[93] All clinical assessments were performed without knowledge of the MRI findings.

The scheme of the whole clinical and radiologic protocol is shown in Figure 10.
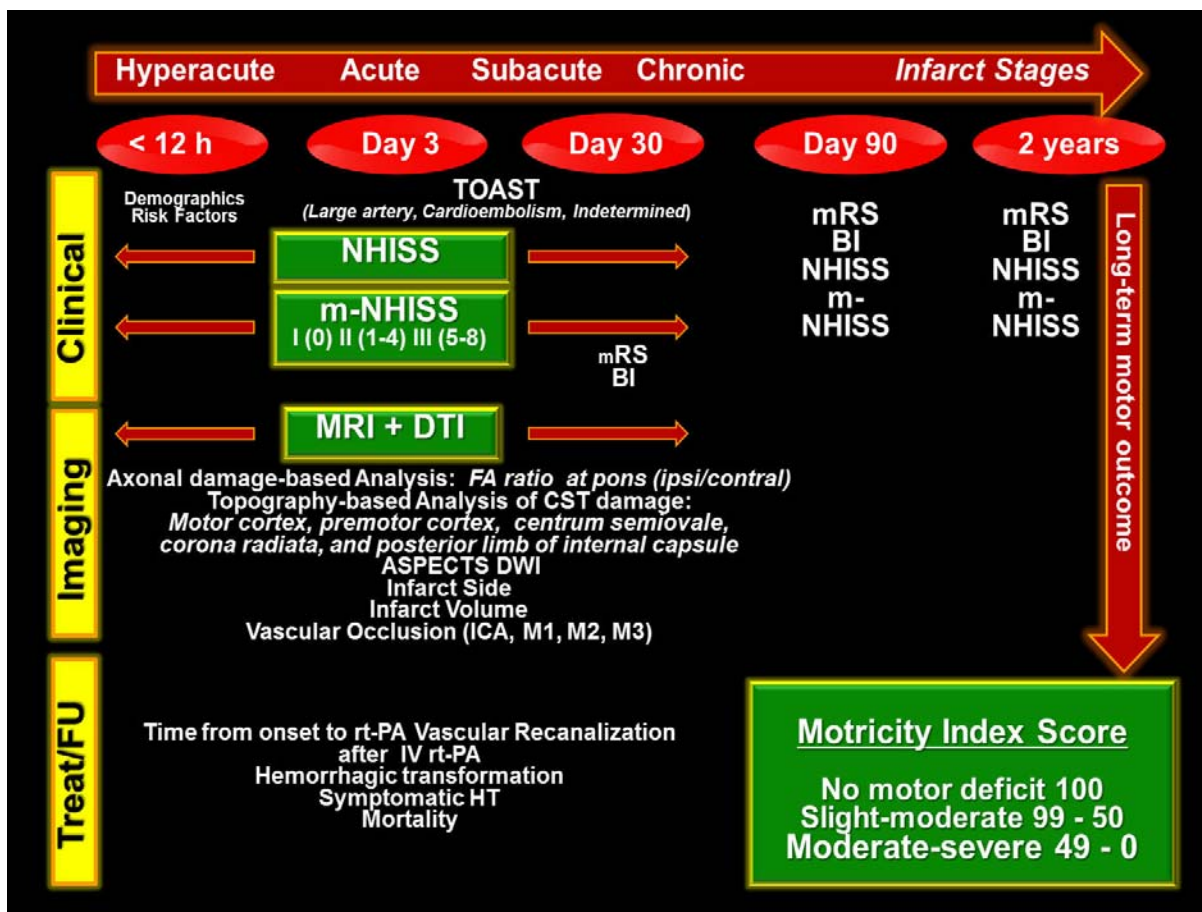
Figure 10. Clinical and MRI protocol from patient's admission to 2 years follow-up.

4.2.3. MRI protocol

All patients underwent MRI examination on a 1.5-Tesla scanner (Intera, Philips Healthcare, Best, the Netherlands). The protocol included axial trace diffusion-weighted imaging (DWI), fluid-attenuated inversion recovery (FLAIR), gradient–echo (GE) T2*-weighted, perfusion-weighted imaging (PWI), time-of-flight angiography, and diffusion tensor imaging (DTI) sequences. DTI data were acquired using single-shot echo-planar imaging sequences with the sensitivity-encoding (SENSE) parallel-imaging scheme (acceleration factor 2) after contrast agent administration.

DTI with echo-planar imaging helped reduce scan time and minimize the susceptibility and distortion artifacts typically associated with echo-planar imaging sequences. Diffusion-sensitized gradients were applied along 15 non-collinear directions with a b value of $1000s/mm^2$. Diffusion-weighted b0 images were also obtained.

Other acquisition parameters were repetition time/echo time (TR/TE) 6795/72 ms, field of view 23 x 23-cm, and matrix size 112 x 112. Forty-five contiguous 3 mm axial slices covering the entire brain and brainstem were acquired parallel to the anterior-posterior line. DTI scanning time was 3 minutes 10 seconds.

4.2.4. Data processing

DTI data were transferred to an offline workstation for post-processing and visually checked for quality. Diffusion-encoded, FA-weighted images were elaborated using the calculation scheme proposed by Pajevic and Perpaoli.[72]

Color FA maps were generated following the standard convention (red, left-right; green, anteroposterior; and blue, superior-inferior) (Figure 11).

Quantitative values of FA were obtained by manually placing regions of interest (ROI) on the entire CST area at level of the rostral pons on axial slices (left and right sides) on the basis of the T2-weighted image and anatomic knowledge, using our image display software (DTIweb, version 2.0, http://trueta.udg.edu/DTI/index.html).[73,74]

FA values for each ROI were obtained by averaging all voxels within the ROI on the sides affected and unaffected by the infarct. In each patient, the FA of the CST was derived from the mean value of three contiguous slices (Figure 11).
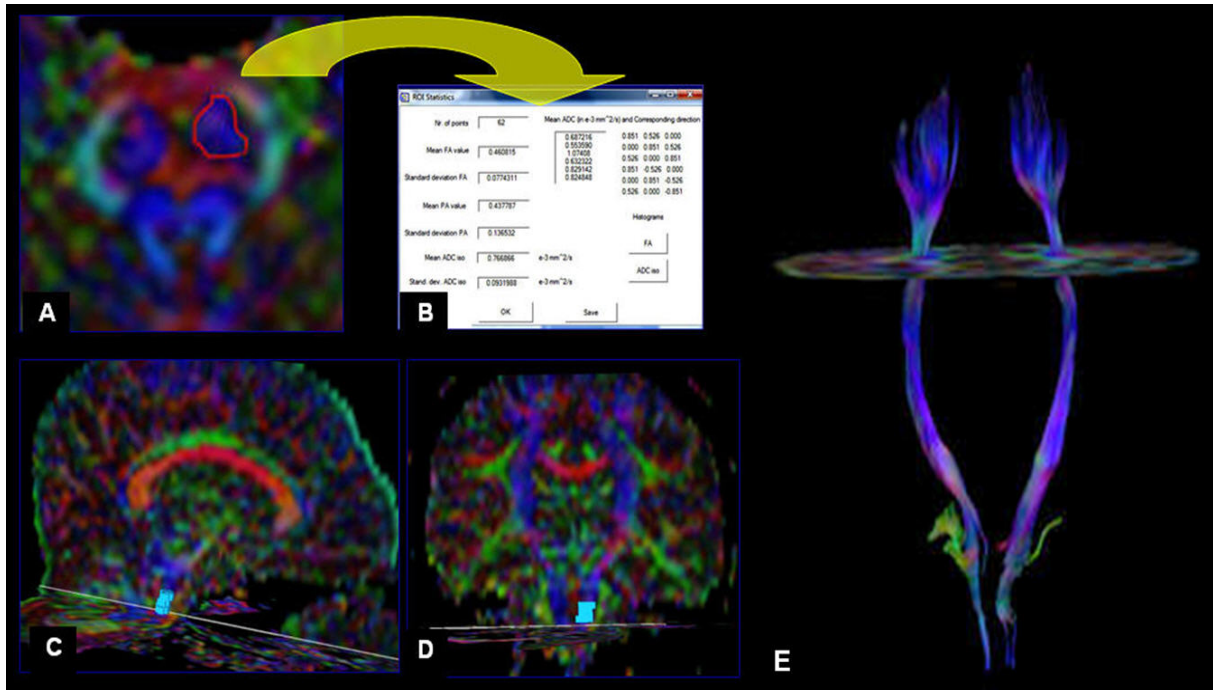
Figure 11. Region of interest assessment (**A**). Example of ROI manual definition in the left cerebral peduncle. (**B**) DTI parameters for each ROI were obtained by averaging all voxels within the ROI on the sides affected and unaffected by the infarct. In this study, the anisotropy of the CST is derived from the mean value of three contiguous slices on sagittal (**C**) and coronal directional maps (**D**). CST tractography reconstruction is represented (**E**).

The ipsilateral-to-contralateral CST FA ratios were calculated (rFA=FAaffected side/FAunaffected side). With this intraindividual evaluation by using rFA, contralateral CST FA values serve as a control.[34]

FA measurements were repeated by one rater on the first thirty patients on the affected and unaffected sides (a total of 180 measurements) on two separate occasions 1 month apart and performed once by two raters. The presented FA values are based on the average of the mean values obtained by two raters.

Statistical analysis (intrarater and interrater comparisions) were performed for the mean FA values. Unaffected CST at the level of rostral pons was used as the internal control for the

assessment of WD-related changes, since no significant differences in anisotropic diffusion are found between tracts on the left and right sides in normal subjects.[74,14]

Signal intensity abnormalities on the affected side of the CST were also determined on diffusion-weighted b1000, T2–weighted, and FLAIR images.

Finally, infarct volumes were evaluated by two raters (JP, GB) manually outlined the areas of abnormal hyperintensity on each slice of diffusion-weighted images. Surfaces of areas of abnormal hyperintensity were summed and multiplied with slice thickness (6mm) and interslice gap (1mm) to calculated infarct volumes. The results of two raters were averaged.

4.2.5. DTI tractography

Tractography was based on a diffusion tensor deflection algorithm.[76] The threshold for stopping fiber propagation was FA < 0.2 and angle < 70º. The seeding method puts randomly inside each voxel with a FA > 0.4.

To reconstruct the CST, the ROIs were placed at the level of the cerebral peduncle and around the CR in the direction-coded color axial sections. Unrelated fibers, such as those going to the contralateral hemisphere, cerebellum, or thalamus, were removed using specific ROIs.

All ROIs were placed by two raters; the CST depicted and the evaluation of the PMC were validated using landmarks from neuroanatomy atlases.[77]
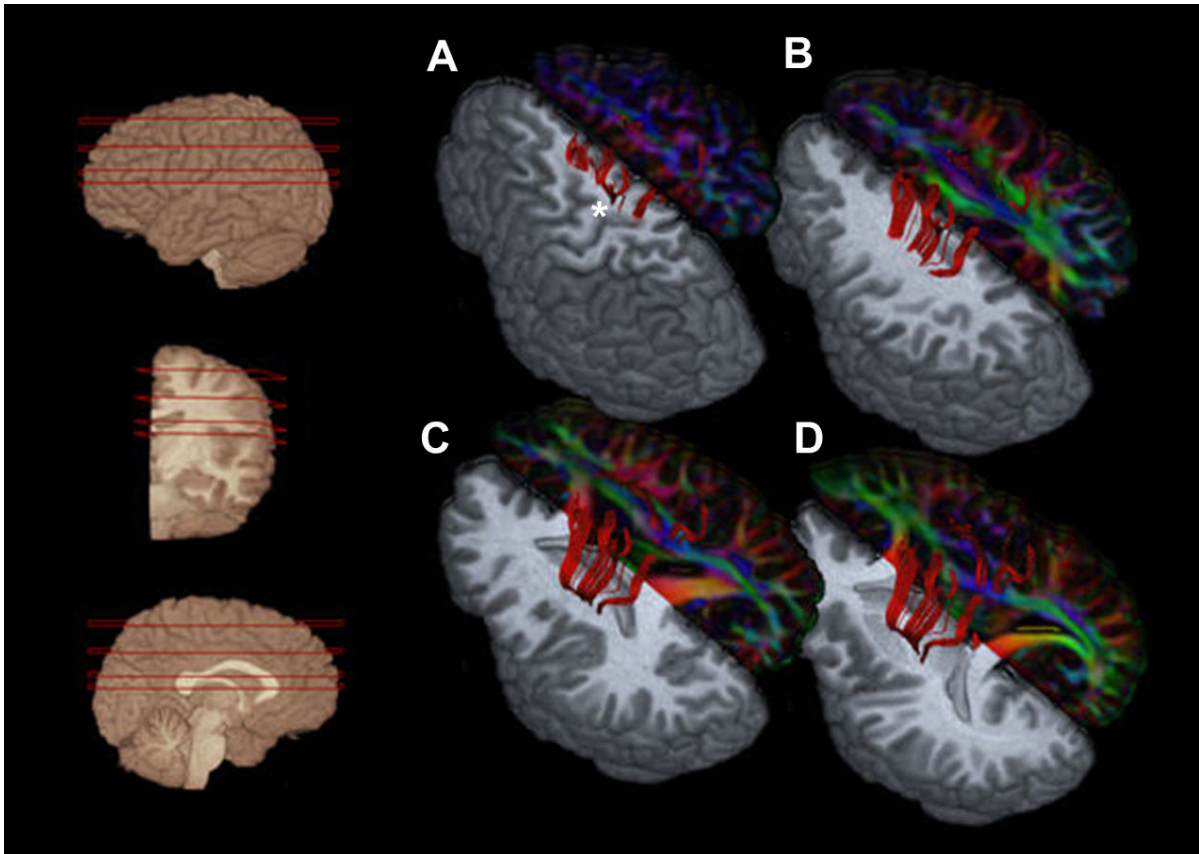
Figure 12. Specific regions evaluated to determine the integrity of the corticospinal tract. Transaxial summed volumetric high-resolution T1-weighted images, FA color-maps, and tractograms show the origin of the corticospinal tract from both the motor cortex (asterisk at precentral gyrus) and primary motor cortex (A). The corticospinal tract involves the centrum semiovale (B) and corona radiate (C) and finally converges at the level of the posterior limb of internal capsule (D). The sectional levels are indicated as red horizontal lines (images on the left).

4.2.6. Assessment of damage to specific corticospinal tract regions

To decide which structures were affected by infarct, the tractograms of CSTs were superimposed on DW images, and the following specific regions were evaluated: MC, PMC, CS, CR, PLIC, and combinations of these regions (Figure 12).

These regions were scored separately on each slice on 2 separate occasions 6 weeks apart by 1 rater and once by 2 raters; all raters were blinded to the clinical ratings. Discordant ratings were resolved by consensus.

4.2.7. Calculation of infarct volume

Infarct volumes were determined offline. Two readers manually outlined the areas of abnormal hyperintensity on axial trace DW images.

Surface areas of abnormal hyperintensity were summed and multiplied by slice thickness (6 mm) and interslice gap (1 mm) to calculate infarct volumes. The results of the two readers were averaged.[34]

4.2.8. Statistical Analysis

The mean and the standard deviation (SD) values for each group were calculated. The statistical evaluation of the results was based on a one-way analysis of variance (ANOVA) with the Bonferroni correction. Levene and Bartlett tests were used to test whether the samples had equal variances, and then ANOVA tests were applied to examine the relationship of mean FA values on the affected side of the CST and of rFA with the clinical scores at admission, at day 3, and at day 30.

To determine the association between mean FA, motor deficit at day 3 and at day 30, and signal change in affected CST, we used the ANOVA test. The Pearson rank correlation coefficient was calculated to compare the FA and rFA values with clinical scores and infarct volumes.

To calculate the FA and rFA cutoff points to discriminate between subjects with motor deficit at day 30 from those without, we used linear discriminant analyses. To determine which variables were associated with motor deficit severity, we used chi-square tests for categorical and ANOVA for quantitative variables.

ROC curves were used to determine rFA cutoffs. Univariate ordinal logistic regression was used to predict long-motor outcome. For these tests, a p-value <0.05 was considered to indicate a statistically significant differences.

To compare first and second measurements of the observer number one (intraobserver reliability) and to compare the measurements of two independent observers (interobserver reliability), intraclass correlation coefficient (ICC) was used. The level of intra and interobserver consistency was classified as fair (ICC=0.5-0.7), good (0.7-0.9) or almost perfect (>0.90). All statistical evaluations were performed using Minitab version 16.1.0.0 (Minitab Inc, State College, Pennsylvania).

5. Results

5.1. Testing whether changes in the anisotropy in the infarct core could detect infarctions up to 4.5 hours of evolution

To test whether DTI-metrics can discriminate ischemic strokes in the first 4.5 hours of onset, we analyzed a cohort of 48 patients (17 women; mean age, 68±14 years) with known onset. Twelve patients with unknown stroke onset time were excluded. Onset was before 4.5 hours in 25 patients (52.1%) with a mean and standard deviation of 182.3 and 65.6 minutes. CST was affected in 35 patients, representing the 72.91% of the sample. Mean ROI area assessed by observers was of 47 mm^2 with standard deviation of 10 mm^2. There were differences between infarcts in the first 4.5 and beyond 4.5 hours for rFA at CST (P=0.001), mean diffusivity radio (rMD) cortical gray matter (P=0.036), rADC cortical gray matter (P=0.009), rT2 at CST (P=0.006), as well as for FLAIR (P<0.001).

In fact, the rFA was increased in the CSTs affected by infarct in the first 4.5 hours. Similarly, rMD and rADC cortical grey matter were also increased in infarcts below 4.5 hours. As expected, FLAIR and rT2WI signal intensity were higher when CSTs were affected beyond 4.5 hours of stroke onset. Figures 13 and 14 show two representative cases of the evolution of rFA and FLAIR signal intensity according the stroke time evolution.

On the other hand, Table 1 clearly summarizes all mean valuables of diffusion metrics and signal characteristics assessed in the study according to stroke evolution.

As a result of statistical analyses carried out a cutoff of 0.970 for rFA was found to discriminate patients before 4.5 hours and beyond 4.5 hours (Figure 15).

Logistic binary regression models and receiver operating characteristic curves demonstrated rFA at CST most reliably discriminated infarcts in the first 4.5 hours (Goodman-Kruskal=0.76;

Kendall=0.39) (Figure 16), with sensitivity, specificity, and positive and negative predictive values for an rFA at CST cutoff of >0.970 being 93.8%, 84.6%, 88.2% and 91.7%, respectively.

Interobserver reliability for ROI measurements and FLAIR rating were good (ICC 0.89 and 0.75, respectively).
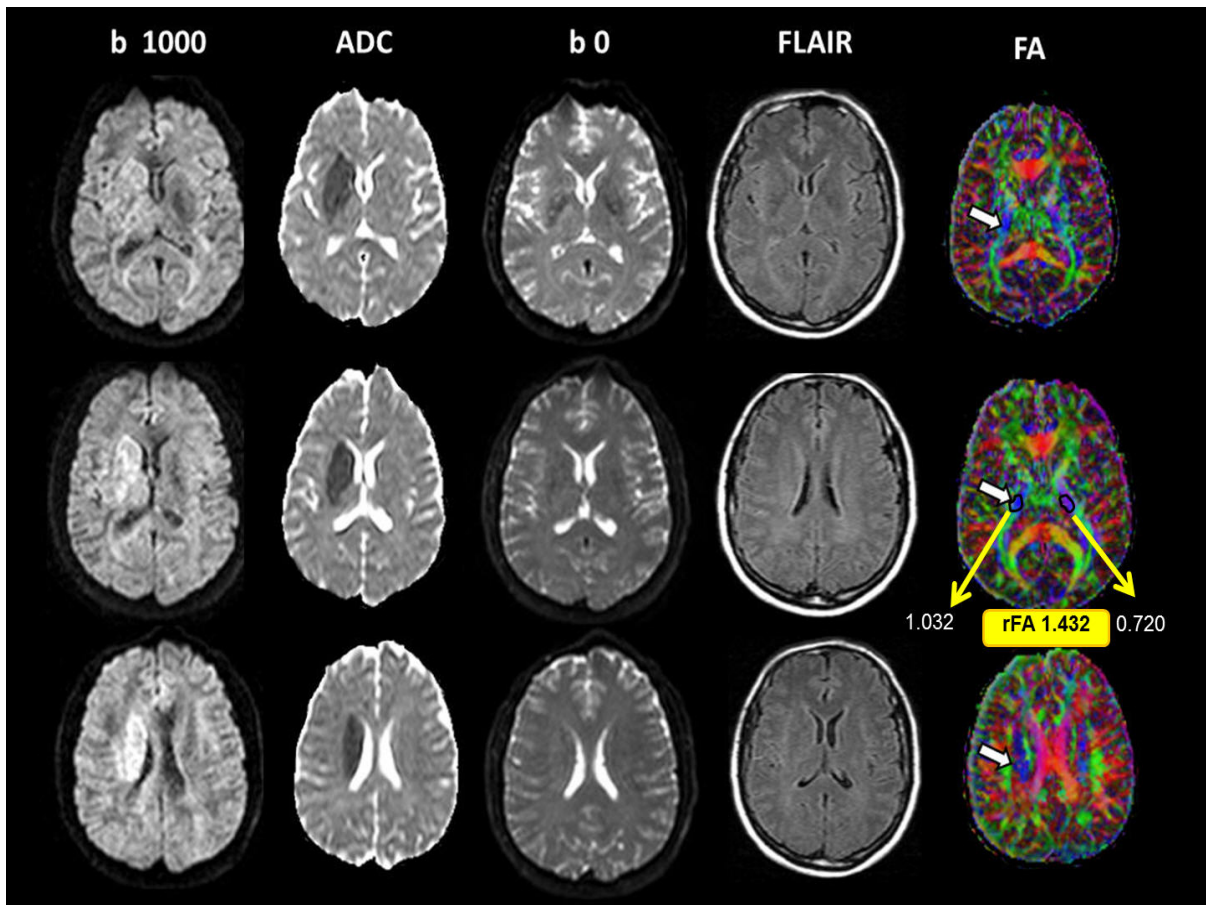
Figure 13. DWI, FLAIR and FA imaging in acute ischemic stroke before 4.5 h of onset (106 min) at the right striatocapsular territory. The color-coded FA map demonstrated slightly increased signal intensity, whereas the FLAIR images and echo-planar T2WI (b0) showed no hyperintensity. This case illustrates how increased FA was not reflected on T2/FLAIR images.
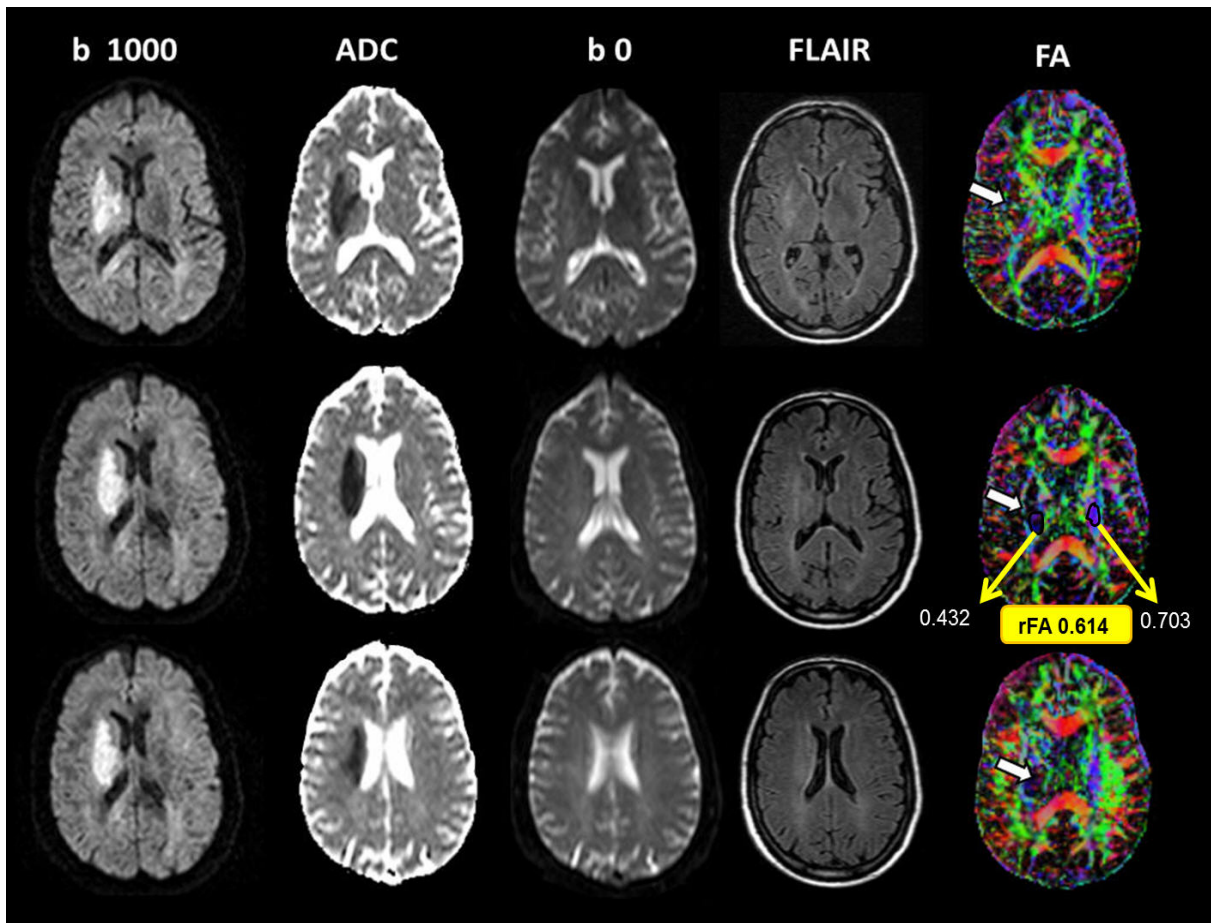
Figure 14. **DWI, FLAIR and FA imaging in acute ischemic stroke > 4.5 h of onset (680 min) involving the right deep MCA territory.** Markedly decreased FA was observed in the PLIC and right corona radiata. This is an example of how decreased FA predicts the stroke onset better than T2/FLAIR images, in which marked signal increase would have been expected (11 h of onset).

Table 1. Diffusion Metrics and Signal Characteristics According to Stroke Evolution

	≤ 4.5 hours (n=25)	> 4.5 hours (n=23)	p-value
Age (years), mean ± SD	66.7 ± 16.0	69.7 ± 13.0	0.485
Gender (Men/Women)	16/9	15/8	0.930
Stroke onset to MRI(min), mean ± SD (n)	182.3 ± 65.6 (25)	485 ± 152 (23)	<0.001
NIHSS score, mean ± SD	10.6 ± 6.36	12.3 ± 6.3	0.315
Stroke mechanism			0.105
Large artery, n (%)	8 (32)	10 (43.5)	
Cardioembolic, n (%)	7 (28)	7 (30.3)	
Indeterminate/other, n (%)	10(40)	6 (26.1)	
FLAIR (normal/hyperintensity) (n)	19/6	5/18	<0.001
rFA cortical GM, mean ± SD (n)	1.209 ± 0.295 (18)	1.064 ± 0.278 (17)	0.146
rFA subcortical WM, mean ± SD (n)	1.189 ± 0.392 (13)	1.416 ± 0.522 (10)	0.247
rFA deep GM, mean ± SD (n)	1.175 ± 0.184 (13)	1.030 ± 0.296 (9)	0.170
rFA CST, mean ± SD (n)	1.178 ± 0.287 (18)	0.826 ± 0.209 (17)	0.001
rMD cortical GM, mean ± SD (n)	0.682 ± 0.122 (13)	0.528 ± 0.212 (11)	0.036
rMD subcortical WM, mean ± SD (n)	0.632 ± 0.148 (13)	0.607 ± 0.180 (8)	0.733
rMD deep GM, mean ± SD (n)	0.695 ± 0.166 (16)	0.728 ± 0.255 (13)	0.679
rMD CST, mean ± SD (n)	0.703 ± 0.235 (18)	0.622 ± 0.248 (17)	0.339
rADC cortical GM, mean ± SD (n)	0.670 ± 0.139 (13)	0.506 ± 0.132 (10)	0.009
rADC subcortical WM, mean ± SD (n)	0.670 ± 0.214 (13)	0.581 ± 0.119 (9)	0.273
rADC deep GM, mean ± SD (n)	0.680 ± 0.185 (16)	0.756 ± 0.206 (12)	0.311
rADC CST,mean ± SD (n)	0.707 ± 0.178 (18)	0.574 ± 0.132 (17)	0.018
rT2WI SI cortical GM, mean ± SD (n)	1.172 ± 0.297 (13)	1.158 ± 0.139 (10)	0.889
rT2WI SI subcortical WM, mean ± SD (n)	1.076 ± 0.218 (13)	1.295 ± 0.397 (8)	0.117
rT2WI SI deep GM, mean ± SD (n)	1.113 ± 0.255 (18)	1.166 ± 0.242 (17)	0.537
rT2WI SI CST, mean ± SD (n)	1.036 ± 0.143 (18)	1.221 ± 0.192 (17)	0.006

NIHSS indicates National Institutes of Health Stroke Scale; r=ratio; FLAIR=fluid-attenuated inversion recovery; FA=fractional anisotropy; GM=gray matter; WM=white matter; MD=mean diffusivity; ADC=apparent diffusion coefficient; T2WI SI=signal intensity on T2-weighted imaging.
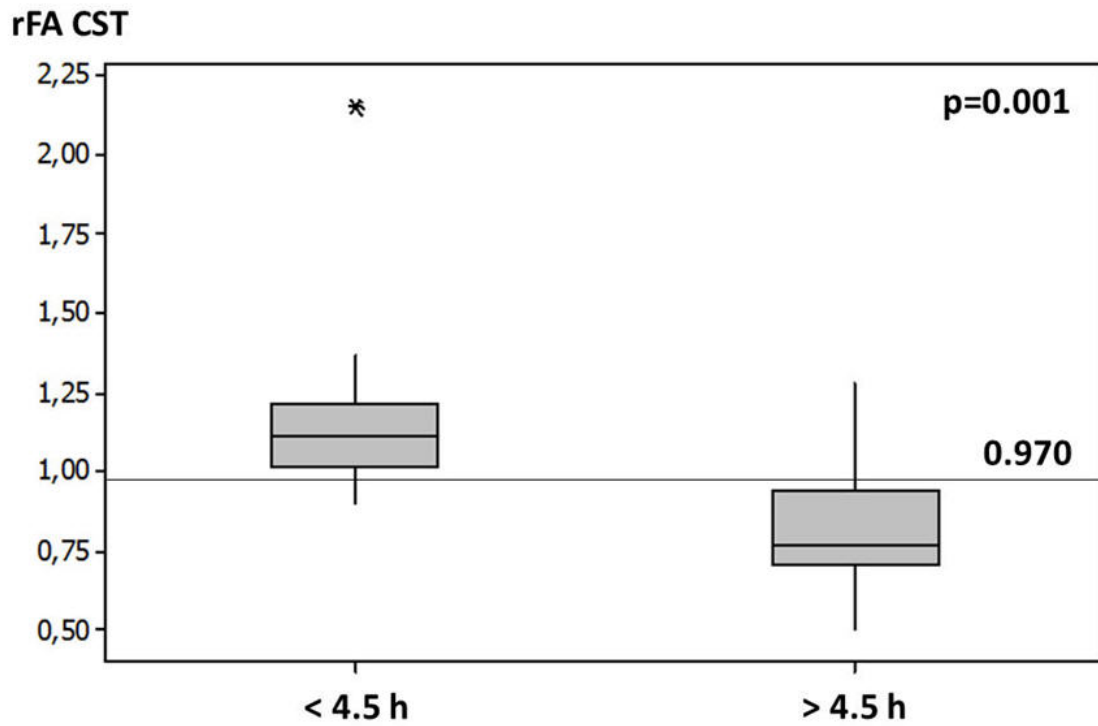
Figure 15. rFA between the affected and unaffected sides at the CST according to time from stroke onset. The line parallel to the x-axis represents the obtained cutoff point that discriminates patients ≤4.5 hours and > 4.5 hours on the basis of rFA. The graph shows medians and quartiles. rFA indicates fractional anisotropy ratio; CST= corticospinal tract.
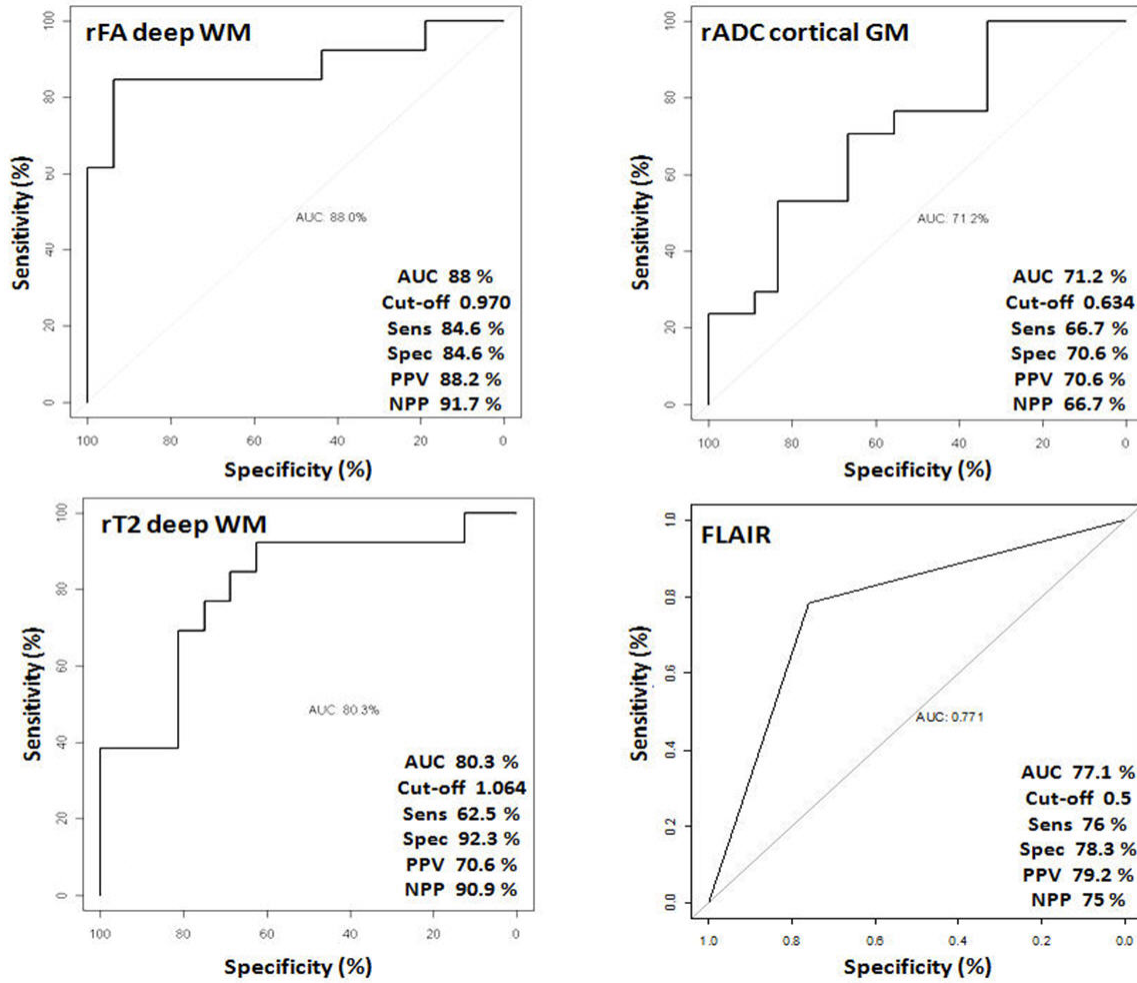
Figure 16. ROC analysis. Area under the curve (AUC), cut-off, sensibility, specificity, positive and negative predictive values for rFA corticospinal tract (deep white matter), rADC cortical gray matter, rT2 corticospinal tract and FLAIR. The highest AUC of these imaging parameters was for rFA corticospinal tract.

5.2. Testing whether quantification of microstructural damage to white matter following stroke by DTI at month could be an independent predictor of long-term motor outcome.

Tables 2, 3 and 4 reports demographic, clinical, and imaging data. At admission, 53/70 patients had motor deficits, representing the 75.6% of the sample; 38/70 (54.1%) were classified as m-NIHSS III, indicating severe motor deficit.

All patients were mobilized within 72 hours after onset and underwent standard physiotherapy during the next 6 months.

At day 30, a total of 35 patients (50%) presented motor deficits; 15 (21.3%) were classified as m-NIHSS III.

Table 2. Demographical and Clinical Data According to Motor Outcome at 2 Years Follow-up

	Overall (N=70)	MI 100 (N=39, 55.7%)	MI 99 - 50 (N=18, 25.7%)	MI < 50 (N=13, 18.6%)	P-value
Demographics					
Age, median (IQR)	72 (61-78.3)	71 (61-79)	67 (51.8-76.5)	75 (70.5-80)	0.481
Female , n (%)	28 (40.0%)	13 (33.3%)	8 (44.4%)	7 (53.8%)	0.385
Risk factors					
Hypertension, n (%)	34 (60.7%)	17 (58.6%)	9 (56.2%)	8 (72.7%)	0.653
Diabetes, n (%)	9 (16.1%)	7 (12.5%)	2 (13.6%)	0 (0%)	0.161
Smoking, n (%)	18 (32.1%)	8 (27.6%)	7 (43.8%)	3 (27.3%)	0.501
Hyperlipidemia, n (%)	27 (48.2%)	14 (48.3%)	6 (37.5%)	7 (63.6%)	0.410
Atrial fibrillation, n (%)	12 (21.4%)	7 (24.1%)	4 (25%)	1 (9.1%)	0.537
Hyperglycemia, n (%)	24 (42.9%)	12 (41.4%)	5 (31.2%)	7 (63.6%)	0.097
Stroke etiology (TOAST)					0.177
Large artery, n (%)	14 (25%)	7 (24.1%)	3 (18.8%)	4 (36.4%)	
Cardioembolic, n (%)	26 (46.4%)	13 (44.8%)	6 (37.5%)	7 (63.6%)	
Indeterminate/other, n (%)	16 (28.6%)	9 (31%)	7 (43.8%)	0 (0%)	

Table 3. Clinical and Imaging Data According to Motor Outcome at 2 Years Follow-up

	Overall (N=70)	MI 100 (N=39, 55.7%)	MI 99 - 50 (N=18, 25.7%)	MI < 50 (N=13, 18.6%)	P-value
Clinical and Imaging Data					
Infarct side, right n (%)	29 (41.4%)	14 (35.9%)	6 (33.3%)	9 (69.2%)	0.077
Total NIHSS scores, median (IQR)					
Admission	12 (6-18)	9 (5-12)	15.5 (10.3-20)	19 (16-20)	<0.001
Day 3	5.5 (1.8-11.3)	2 (1-4)	8 (6-13.5)	17 (12-19)	<0.001
Day 30	2 (0-9)	1 (0-2)	5 (2-10)	16 (10-19)	<0.001
Day 90	2 (0.8-4)	1 (0-2)	2.5 (1-4)	14 (4-4)	<0.001
Year 2	0 (0-6.3)	0 (0-0)	1 (0.8-6.5)	13 (10-14)	0.001
m-NIHSS scores, median (IQR)					
Admission	4.5 (1-8)	2 (0-5)	7 (1.8-8)	8 (7-8)	<0.001
Day 3	0 (0-5)	0 (0-0)	3 (0.8-5.5)	8 (6-8)	<0.001
Day 30	0 (0-4)	0 (0-0)	3 (0-4.3)	7 (5.5-8)	<0.001
Day 90	0 (0-4)	0 (0-0)	1 (0-4.3)	7 (5.5-7)	<0.001
Year 2	0 (0-3)	0 (0-0)	1 (0-3)	7 (6-7.5)	<0.001
FA at admission, median (IQR)					
Affected side	0.61 (0.65-0.61)	0.6 (0.64-0.6)	0.64 (0.66-0.64)	0.63 (0.67-0.63)	0.967
Unaffected side	0.61 (0.65-0.61)	0.61 (0.64-0.61)	0.61 (0.68-0.61)	0.61 (0.65-0.61)	0.935
FA at day 3, median (IQR)					
Affected side	0.62 (0.65-0.62)	0.62 (0.65-0.62)	0.63 (0.69-0.63)	0.6 (0.64-0.6)	0.393
Unaffected side	0.61 (0.65-0.61)	0.61 (0.64-0.61)	0.63 (0.67-0.63)	0.61 (0.64-0.61)	0.251
FA at day 30, median (IQR)					

Affected side	0.57 (0.63-0.57)	0.61 (0.67-0.61)	0.52 (0.59-0.52)	0.38 (0.42-0.38)	<0.001
Unaffected side	0.62 (0.65-0.62)	0.60 (0.64-0.6)	0.62 (0.66-0.62)	0.64 (0.68-0.64)	0.015
rFA					
Admission	1.01 (1.05-1.01)	1 (1.05-1)	0.98 (1.08-0.98)	1.02 (1.05-1.02)	0.282
Day 3	1.01 (1.05-1.01)	1.01 (1.05-1.01)	1.01 (1.05-1.01)	1 (1.04-1)	0.429
Day 30	0.98 (1.02-0.98)	1.02 (1.07-1.02)	0.91 (0.94-0.91)	0.59 (0.63-0.59)	<0.001
Location of CST damage, admission, n (%)					
Motor cortex	18 (25.7%)	8 (20.5%)	3 (16. 7%)	7 (53.8%)	0.035
Premotor cortex	15 (21.4%)	7 (17.9%)	4 (22.2%)	4 (30.8%)	0.619
Centrum semiovale	12 (17.1%)	4 (10.3%)	2 (11.1%)	6 (46.2%)	0.009
Corona radiata	35 (50.0%)	14 (35.9%)	2 (66.7%)	9 (69.2%)	0.030
PLIC	14 (20.0%)	0 (0.0%)	6 (33.3%)	8 (61.5%)	<0.001
Location of CST damage day 3, n (%)					
Motor cortex	18 (25.7%)	8 (20.5%)	3 (16.7%)	7 (53.8%)	0.035
Premotor cortex	19 (27.1%)	8 (20.5%)	4 (22.2%)	7 (53.8%)	0.056
Centrum semiovale	17 (10.3%)	4 (27.8%)	5 (61.5%)	8 (24.3%)	0.001
Corona radiata	39 (55.7%)	13 (33.3%)	14 (77.8%)	12 (92.3%)	<0.001
PLIC	17 (24.3%)	0 (0.0%)	8 (44.4%)	9 (69.2%)	<0.001
Location of CST damage day 30, n (%)					
Motor cortex	16 (22.9%)	6 (15.4%)	3 (16.7%)	7 (53.8%)	0.013
Premotor cortex	17 (24.3%)	8 (20.5%)	2 (11.1%)	7 (53.8%)	0.017
Centrum semiovale	18 (25.7%)	4 (10.3%)	5 (27. 8%)	9 (69.2%)	<0.001
Corona radiata	39 (55.7%)	14 (35.9%)	13 (72.2%)	12 (92.3%)	<0.001
PLIC	17 (24.3%)	0 (0%)	8 (44.4%)	9 (69.2%)	<0.001
Infarct volume, median (IQR)					
Admission	9.2 (4.8-24.7)	7 (4.4-15.5)	12.3 (4.8-23.5)	24.5 (14.7-70.9)	0.004

Day 3	19.1 (9.2-53.5)	10.4 (7.1-22.6)	26.1 (14-61.3)	83.7 (41.5-148.8)	<0.001
Day 30	10.1 (4.1-40.3)	7.5 (3.2-11.3)	15.1 (7.5-49)	69.4 (31.8-120.2)	<0.001
Year 2	0 (0-2.3)	0 (0-0)	1 (0-2.3)	4 (3-4.5)	<0.001

Table 4. Outcome Data According to Motor Outcome at 2 Years Follow-up

	Overall (N=70)	MI 100 (N=39, 55.7%)	MI 99 - 50 (N=18, 25.7%)	MI < 50 (N=13, 18.6%)	*P*-value
IV rt-PA treatment, n (%)	36 (41.4%)	20 (51.3%)	8 (44.4%)	8 (61.5%)	0.643
Time onset to IV rt-PA, min, median (IQR)	170.5 (150-191.3)	170 (154-180)	184.5 (117.5-210)	150 (145-230)	0.729
Recanalization after IV rt-PA, n (%)	14 (38.9%)	5 (26.3%)	3 (30%)	6 (85.7%)	0.018
Hemorrhagic transformation, n (%)	25 (44.6%)	8 (27.6%)	11 (68.8%)	6 (54.5%)	0.022
mRS, median (IQR)					
Day 30	2 (1-4)	2 (1-2)	3 (2.8-4)	4 (4-4)	<0.001
Day 90	1 (1-2)	1 (0-1)	2 (1-2.5)	4 (3-4)	<0.001
Year 2	0 (0-2.3)	0 (0-0)	1 (0-2.3)	4 (3-4.5)	<0.001
BI Score, median (IQR)					
Day 30	100 (48.8-100)	100 (100-100)	82.5 (45-100)	25 (22.5-42.5)	<0.001
Day 90	100 (63.8-100)	100 (100-100)	92.5 (57.5-100)	35 (25-40)	<0.001
Year 2	100 (77.5-100)	100 (100-100)	100 (77.5-100)	40 (20-45)	<0.001
MI Score at 2 years, median (IQR)					
Global	100 (61-100)	100 (100-100)	84 (61-91)	25 (4.5-28.5)	<0.001
Upper extremity	100 (39-100)	100 (100-100)	84 (39-91)	15 (2.3-29)	<0.001
Lower extemity	100 (83-100)	100 (100-100)	84 (83-91)	32 (6.8-34.5)	<0.001

At 2-year follow-up, 31 patients (44.3%) presented motor deficits and 13 (18.6%) presented Motricity Index score <50.

Interestingly, 14 patients (20%) had involvement of the PLIC on admission; all these presented some motor deficit at 2-year follow-up (P<0.001) (Figure 17). In this respect, none of patients with normal motor function presented PLIC damage.

On the other hand, 44.4% and 69,2% of patients with moderate and severe motor deficit at 2-years follow-up presented PLIC affected by infarct on admission.
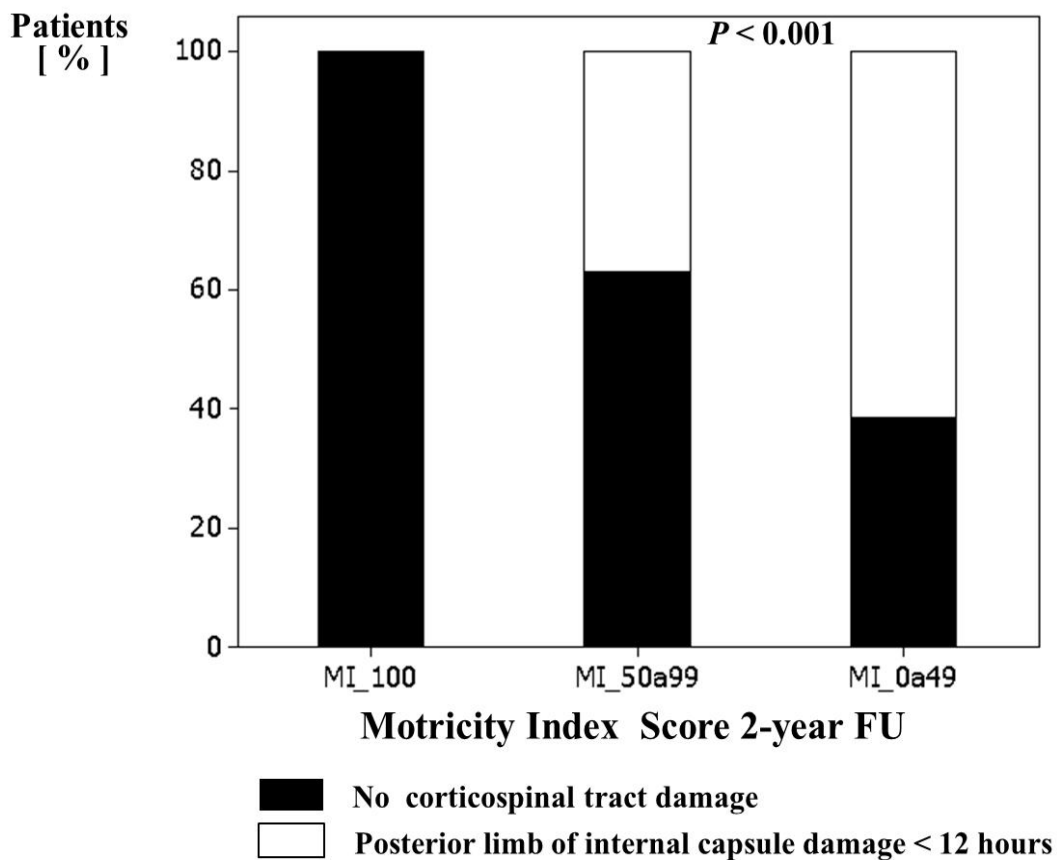
Figure 17. Influence of posterior limb of internal capsule damage and long-term motor evolution at 2-years follow-up.

Infarct volume at admission, day 3, and day 30 correlated with motor deficit severity at 2 years (Figure 18).
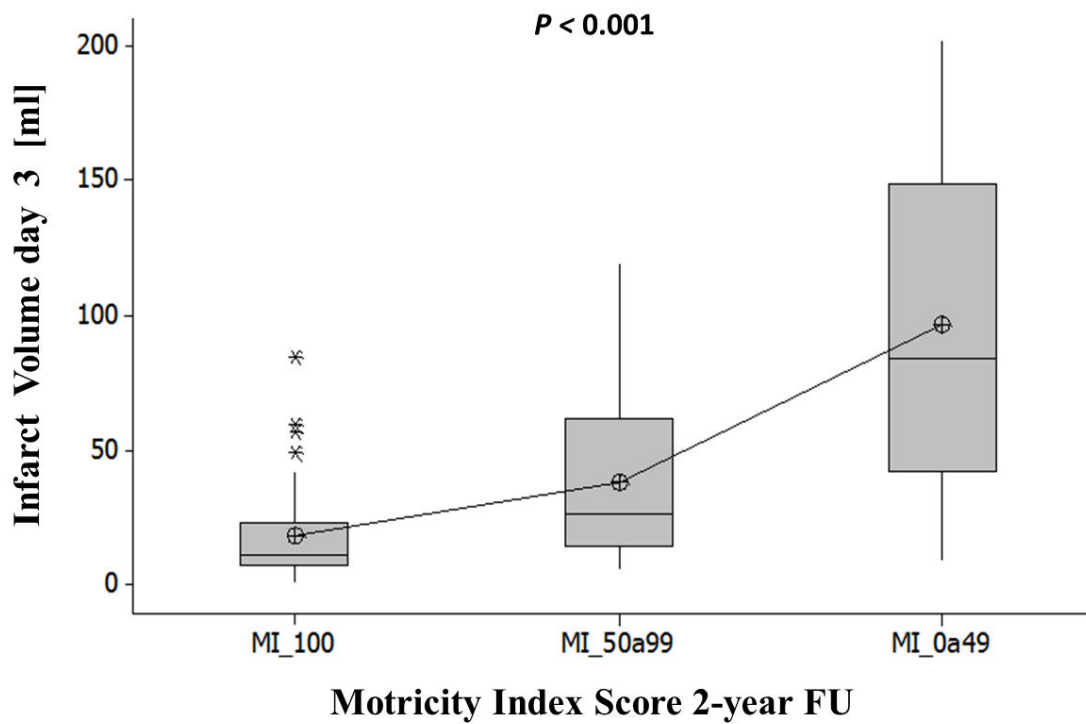
Figure 18. Associations between infarct volume at day 3 and long-term motor outcome at 2 years after stroke.

Mean FA values in affected CST at the pons at day 30 decreased progressively in line with increasing motor deficit at 2-year follow-up (P<0.001).

The rFA cutoff points distinguish patients without motor deficit at 2-year follow-up from those with slight-moderate deficit and even differentiate the latter from patients with severe motor deficits (Figure 19).

The rFA cutoffs <0.982 for slight-moderate and <0.689 for severe motor deficit at 2 years yielded sensitivity 94.4% and 84.6%, specificity 73.9% and 97.1%, positive predictive value 100% and 83.3%, and negative predictive value 81.3% and 100%, respectively.
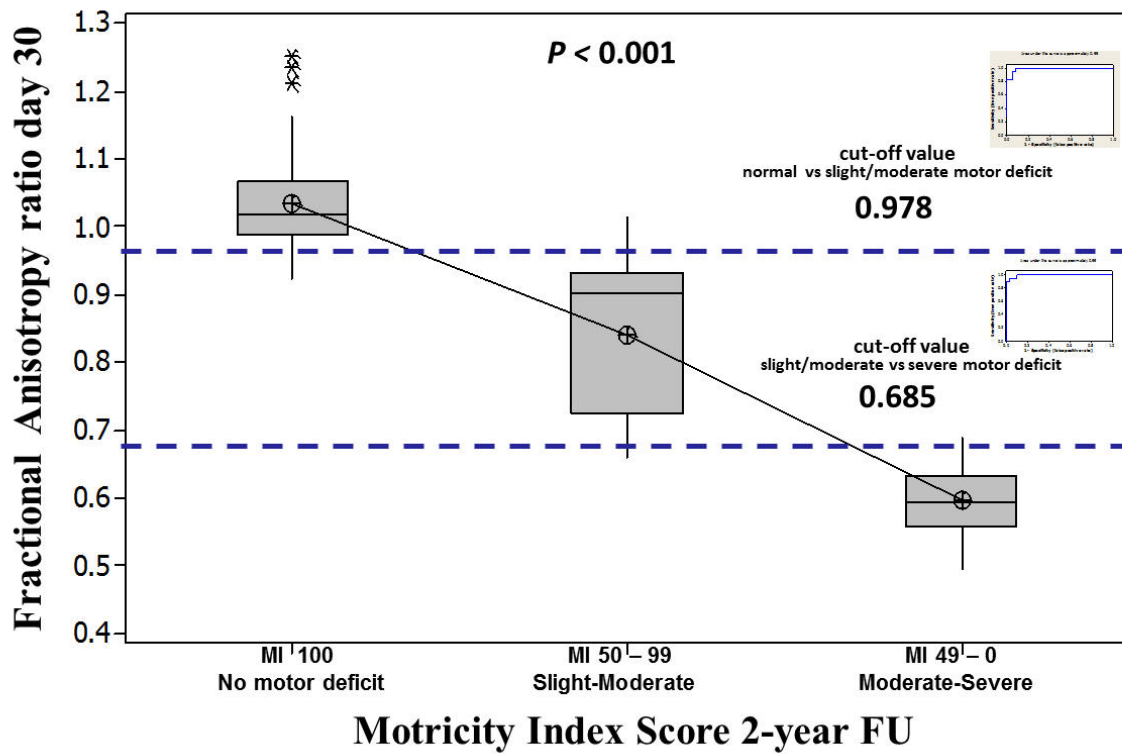
Figure 19. Associations between axonal damage at day 30 and long-term motor outcome at 2 years after stroke.

Table 5. Table of correlations between motor deficit at day 30, axonal damage and long-term motor outcome at 2 years after stroke

	2 years			
	MI 100 *No motor deficit* *(N=39, 55.7%)*	*MI 50 – 99* *Slight-Moderate* *(N=18, 25.7%)*	*MI 49 - 0* *Moderate-Severe* *(N=13, 18.6%)*	*Overall* *(N=70)*
Day 30				
m-NIHSS I *No motor deficit*	38 mean rFA (SD) 1.037 (0.077)	7 mean rFA (SD) 0.931 (0.096)	0 mean rFA (SD) NA (NA)	45 mean rFA (SD) 1.020 (0.088)
m-NIHSS II *Slight-Moderate*	1 mean rFA (SD) 1.001 (NA)	7 mean rFA (SD) 0.821 (0.107)	2 mean rFA (SD) 0.673 (0.020)	10 mean rFA (SD) 0.816 (0.127)
m-NIHSS I II *Moderate-Severe*	0 mean rFA (SD) NA (NA)	4 mean rFA (SD) 0.737 (0.105)	11 mean rFA (SD) 0.581 (0.045)	15 mean rFA (SD) 0.623 (0.994)
Overall	39 mean rFA (SD) 1.036 (0.076)	18 mean rFA (SD) 0.849 (0.123)	13 mean rFA (SD) 0.595 (0.054)	70 mean rFA (SD) 0.906 (0.189)

In each cell the number of cases with its mean and standard deviation of the rFA is provided

After adjusting for other variables related to motor outcome, statistical models show that rFA at day 30 was the only predictor of motor outcome at 2 years with an odds ratio of 1.60 and 95% confidence interval ranged from 1.26 to 2.03 (P<0.001) (Table 6).

Table 6. Model Selected from Ordinal Logistic Regression Analysis for Predicting Long-term Motor outcome 2 years After Stroke

Predictor	Regression Coefficient	Z	*P*-value	Odds Ratio	95% CI
rFA day 30	0.472	3.90	<0.001	1.60	1.26-2.03
Infarct volume day 3	-0.023	-1.47	0.142	0.98	0.97-1.01
m-NIHSS II day 30	-0.240	-0.14	0.887	0.79	0.03-21.33
m-NIHSS III day 30	2.342	0.85	0.394	10.40	0.05-22.60
PLIC damage at admission	-2.808	-1.35	0.177	0.06	0.00-3.57
Constant (1)	-44.872	-3.83	<0.001	NA	NA
Constant (2)	-31.607	-3.89	<0.001	NA	NA

6. Discussion

6.1. The role of anisotropy in determining the time of stroke onset

To my knowledge, this is the first study demonstrating that rFA at CST increased in the first 4.5 hours; more specifically, an rFA over 0.970 reliably predicted whether before 4.5 hours had elapsed since onset. Serial longitudinal studies of animal models of cerebral ischemia have shown that FA is elevated (up to 20%) within the first 5 hours of onset in rats and monkeys but then declines over the ensuing time course. [18,70]

In patients with acute ischemic stroke, increased FA within the first day of stroke has been observed, but this finding is not consistent: several other studies report reductions or no change in FA over the same time frame.[71-78-80] The precise cause of the increase in anisotropy is not well understood, but a previous simulation study indicated that it is cellular membrane failure that restricts transverse diffusivity in the hyperacute stage of infarction.[16] Oligodendrocyte swelling from cytotoxic edema, one of the earliest morphological changes after stroke, results in extraaxonal water and compression of the axoplasm by swollen myelin sheaths, which translates to greater decline in radial than axial water diffusivity in infarcted white matter and increased rFA.[16,17]

Although the cellular basis of this phenomenon is not completely clear, it could explain the increase in FA ratios (rFA) in the first hours. The current findings of this thesis elevated FA in hyperacute stroke are consistent with previous studies.[11,17-21,70] As the infarct evolves over time, the breakdown of the axons eventually results in massive water accumulation in axon tracts that translates to hyperintensity in FLAIR and T2-weighted images.[20] In the hyperacute stage, large decreases in FA suggest loss of cellular integrity with irreversible axonal injury not reflected on conventional MRI.

Significant FA alterations only in the CST were detected, probably attributable to the greater anisotropy of the tightly packed single-directed fibers. A recent cross-sectional DTI study of ischemic white matter regions showed that FA was significantly elevated (up to 25%) only ≤7 hours

of symptom onset and then decreased consistently (∼15% declines) from 8 h to 34 h after stroke.[19] Using anisotropy parameters in the lesion relative to the contralateral side, one study showed elevated FA ratios mainly within 24 hours, whereas reduced rFA occurred primarily after 24 h.[21] Another study showed a reduced and constant rFA in white matter and gray matter, respectively.[71]

6.2. The role of DTI in predicting motor outcome in stroke patients

Motor deficit is one of the most common sequelae of ischemic stroke, and its severity correlates with functional disability and reduced quality of life.[22] The CST is the most important motor pathway.[81]

The extent of wallerian degeneration (WD) in the CST is one of the major determinants of motor deficit.[82] WD consists of the anterograde degeneration of axons and their myelin sheaths after proximal axonal or cell body injury from numerous causes, including stroke. Many studies have reported hyperintense signals regarded as WD along the affected CST on T2-weighted or diffusion-weighted imaging weeks or months after stroke, and this finding correlates well with persistent functional disability.[83-86] However, on conventional MRI, these findings are usually subtle and can be difficult to detect in the first few weeks; moreover, the extent of WD is difficult to quantify on conventional MRI and is not consistent in all patients with motor deficit.[34]

Recently, much interest has focused on the potential of DTI for in vivo quantification of microstructural damage to cerebral white matter following stroke. Reduced anisotropy along the CST remote from a cerebral infarct has been interpreted as WD, even when these areas appeared normal on conventional MRI.[87,88] In this line, after assessing WD changes qualitatively on conventional images and quantitatively by using DTI, we found differences in anisotropy in patients with motor deficits who had no signal-intensity abnormalities on conventional MRI.[34]

Most important, most patients with motor deficits at 30 days who presented decreased FA values had no signal-intensity abnormalities on the affected side of the CST; more specifically, fewer than half presented hyperintensities on FLAIR and/or restricted diffusion on DWI. The signal-intensity change in the affected CST was strongly associated with lower FA indexes. These findings suggest that DTI is more sensitive in detecting tissue changes regarded as WD than conventional MRI and DWI.

Of note, the results of this thesis shown that lower rFA at day 30 was strongly associated with poor outcome and 2 cutoffs predicted motor deficit severity. Motor deficit on admission, infarct volume and location, as well as CST damage have been proposed as predictors of motor outcome.[24,25,27,34] Although greater initial motor impairment predicts worse motor recovery, the relation varies widely among subjects, and accurate prognosis remains difficult.

On the other hand, volume infarct measures do not take into account the location of the lesion or the functional pathways involved, and two infarcts of the same size in different locations could have very different functional expression.[48] Thus, rather than total stroke lesion volume, it seems much more reliable to use DTI to evaluate the extent of damage specifically within the CST to determine motor deficit and axonal injury.[34] The current findings corroborate the findings of other cross-sectional studies that lower FA values in the affected CST were associated with greater motor deficit in the first week after stroke and worse motor outcome at 3 months, indicating motor outcome strongly depends on CST integrity.[34,33,38-42,89]

In an experimental model after unilateral MCA occlusion in rats, signs of WD in the CST were detected in the brain stem in histologic stains as early as 2–7 days after the stroke.[43] Within the second stage, WD decreased gradually up to 6 weeks. Other recent studies have demonstrated early signs of WD in patients with stroke within 2–3 weeks of onset by using DTI.[15,41] Greater FA

reduction along the CST on the affected side after cerebral infarction is associated with greater early motor deficit and worse motor recovery at 3 months.[33,37-39]

In this research, significant correlations were found between FA indexes and motor deficit only at 30 days, and the reductions in mean FA, 17% and 32% in patients with m-NIHSS-II and m-NIHSS-III respectively, are similar to other published values measured at the pons.[14,88] Thomalla et al.[87] found a 13% decrease in FA measured at the cerebral peduncle 2–6 months and 2–16 days after stroke. Severe WD in the CST distal to a supratentorial infarct in the acute stage has been regarded as a predictor of worse motor outcome.[33,38-42,87-89] Liang et al.[41] conducted a similar longitudinal controlled study by using serial DTI to assess both antegrade and retrograde WD in 12 patients with subcortical ischemic infarctions involving the posterior limb of the internal capsule. They found progressive decrease in FA with time starting from the first week in the region just proximal and distal to the internal capsule lesion. On the other hand, Wanatabe et al.[42] used serial DTI evaluations to assess WD in the CST of 16 patients with stroke (6 ischemic, 10 hemorrhagic). They found that the good recovery group had no significant change in anisotropy in the rostral pons between 2 and 3 weeks, whereas the poor recovery group had a significant decrease in anisotropy during that time. Although not specifically calculated, Fig 4 of their study shows that the 0.9 ratio is the approximate anisotropy cutoff for distinguishing the separate recovery groups 3 weeks after onset.

More than 50% of patients require specialized rehabilitation after stroke.[90] However, rehabilitation is expensive, and its success depends on careful patient selection. Early information from rFA analysis might help tailor rehabilitation. Patients with lower rFA are less likely to benefit from active rehabilitation. Future rehabilitation trials might enable better selection of strategies for individual patients on the basis of the integrity of the motor system.

One new research line aims to improve neurologic outcome through stem cell-based treatment of chronic stroke.[91] Although the study of the mechanisms underlying stem cell-based

treatment has focused on angiogenesis and neurogenesis, white matter reorganization may contribute to functional recovery after stroke. The earliest stem cell transplantations were carried out 4–9 weeks from onset,[92] and 4 weeks was also the time when our study demonstrated CST damage in the patients with motor deficits.

DTI may also be useful in determining the real state of the CST before treatment, quantifying the amount of damage specifically within the motor system after stroke, and FA indexes could be an alternative way of monitoring the changes in cerebral tissue that lead to improved outcome.

The current research has certain limitations. Our relative small sample limits the power of our findings. The rFA cutoff value was not applicable to other regions of territorial infarction, although almost three-quarters of patients had CST damage. Analyzing radial diffusivities might provide additional information about stroke time. Further studies in acute stroke patients are required to assess whether DTI quantification improves the determination of stroke onset time and is useful in treatment decision making. The m-NIHSS scores obtained in acute phase are not especially sensitive for limb motor impairment, and a more specific score administered at 30 days might better predict long-term motor outcome. Tract-specific FA or voxel-based analysis might outperform FA of predetermined regions of interest. Quantifying infarct overlap with the CST on DTT by voxel-based analysis might help predict motor outcome. Future studies should include more patients with various stroke types and locations, compare MRI outcome markers to others like NIHSS scale, and analyze other DTI-metrics.

7. Conclusions

The main conclusions of this research can be summarized as follows:

A) Our research suggests that microstructural changes attributable to ischemia at CST by DTI-metric rFA can reliably discriminate ischemic strokes between ≤ 4.5 hours and > 4.5 hours of onset. The rFA at CST could play a role as a biological tissue clock in patients with territorial MCA stroke.

B) The sensitivity, specificity, and positive and negative predictive values for infarct ≤ 4.5 hours of onset by rFA at CST > 0.970 were 93.8%, 84.6%, 88.2%, and 91.7%, respectively. All these points lead to the conclusion that the FA could be used as MRI surrogate marker of lesion age.

C) DTI-metrics at CST correlate with long-term motor outcome and provide accurate prediction of long-term motor deficit after stroke. This was particularly noteworthy as regards rFA at day 30 is an independent predictor of long-term motor outcome after MCA ischemic stroke.

D) The sensitivity, specificity, and positive and negative predictive values of the cutoffs rFA at CST < 0.982 at day 30 for predicting slight-moderate deficit and rFA < 0.689 for severe deficit were 94.4%, 84.6%, 73.9%, and 97.1%, respectively, and 100%, 83.3%, 81.3%, and 100%, respectively at 2-years follow up. Therefore, the rFA values at day 30 could potentially be used as an imaging surrogate marker for long-term motor deficit.

8. Future

Understanding brain connectivity is an international research priority.[94] The brain is a complex network of interacting functionally and structurally connected regions. Indeed, there is a circular relationship between behavioral performance, brain functionality, and neuronal micro- and macro-structural architecture. In recent years, advanced MRI techniques have enabled unique insights into structural and functional bran connectivity.[95]

Whereas DTI has proved useful for studying the macrostructure and microstructure of the brain,[35] functional MRI has revolutionized our understanding of the location of specific cognitive domains and behavioral processes.[96] Changes in tissue microstructure are often the earliest signs of neurologic diseases or the effect of a treatment, but are mostly only measurable using microscopy on excised tissue samples. Advanced MRI biomarkers bring us closer to understanding tissue microstructure and structural connectivity.

Therefore, advanced MRI biomarkers based on DTI like those proposed in this thesis would make it possible to determine the patterns of development in each individual patient, including stimulation aimed at recovering from specific lesions and compensatory rehabilitation and other interventions aimed at improving specific functions.

Observational studies have demonstrated that outcome after stroke is associated with initial neurologic deficit, age, demographics, comorbidities, infarct site, lesion volume, infarct side, and stroke subtype. However, in acute settings, clinical assessment is limited by difficulties in assessing uncooperative or cognitively impaired patients, and clinical prognosis can be inconclusive. Thus, a valid surrogate functional outcome measure for stroke is needed. Diffusion tensor tractography in conjunction with functional MRI could improve prognostic accuracy and help improve patient's management (Figure 20).
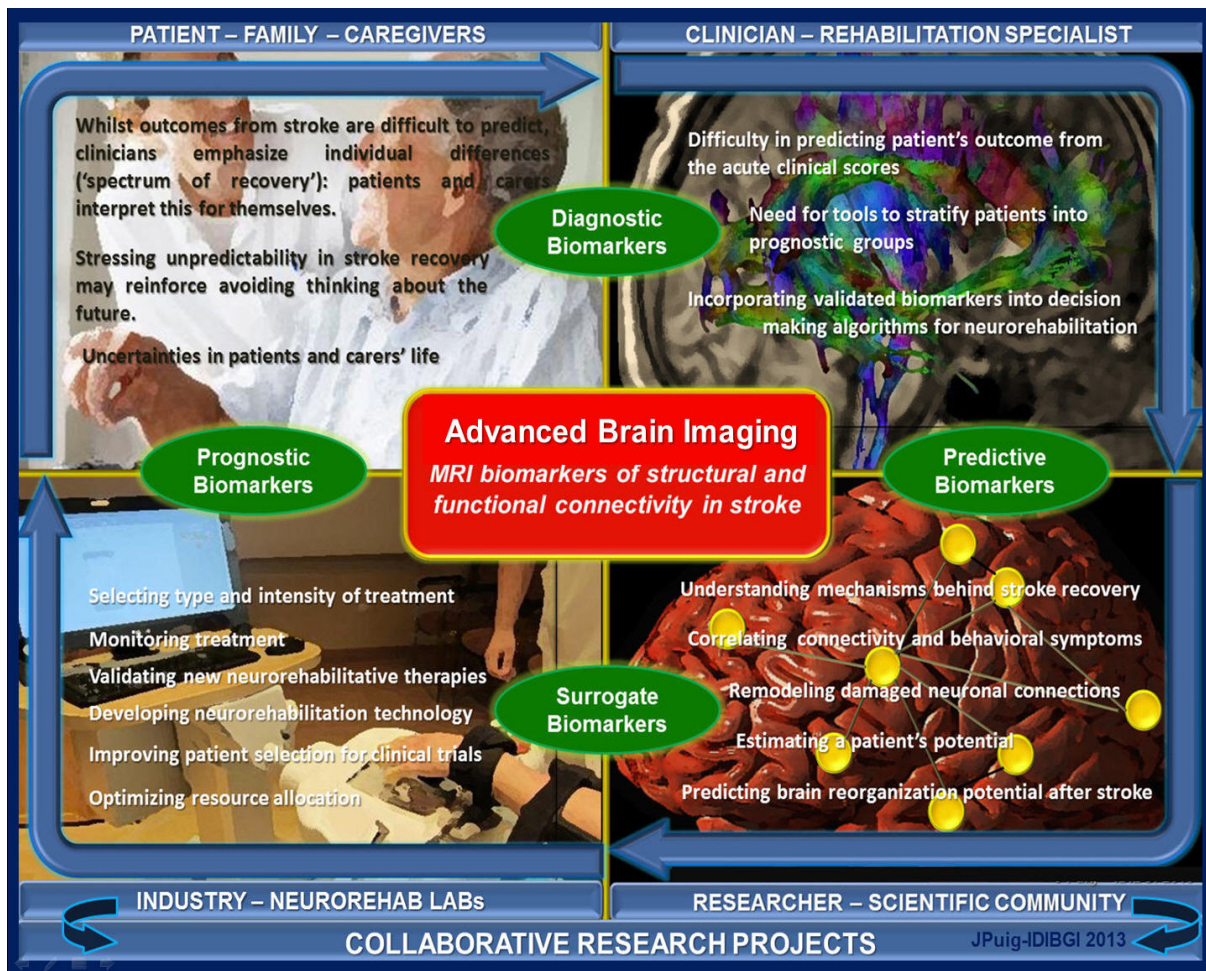
Figure 20. Why MRI connectivity biomarkers matter to society. Stroke strikes many people in developed countries. The assessment of functional and structural architecture of brain networks is critical to understanding the clinical effects and course of post-stroke recovery: MRI connectivity biomarkers would enable patients, family, and caretakers to know what to expect in the early stage of stroke. Incorporating validated biomarkers into decision-making algorithms for neurorehabilitation might help more patients benefit from rehabilitation, because evidence-based evaluation of neurorehabilitation treatment approaches might help determine whether potential functional recovery through stimulating neuroplasticity would justify neurorehabilitation strategies. MRI connectivity biomarkers, including DTI-metrics and tractography, would help clinicians and rehabilitation specialists set goals, select the type and intensity of treatment, and ensure the appropriate level of care for each individual patient.

However, this topic is more complex: local damage can result in remote alterations. Similar structural damage results in different levels of functional impairment; patients can have multiple acute deficits not easily attributed to focal lesions. Complex symptoms not explained by direct damage might be explained by effects on distal regions connected to the damaged tissue. The

combination of imaging and clinical measures might be able to predict about 70% to 75% of the variance in outcome at 3 months. The remaining 25% to 30% might be explained by genetic factors, intensity of rehabilitation, psychosocial support, hemisphere affected, or pre-existing small vessel disease or anatomic variability.

Evidence of neural plasticity has grown fast. Robust experimental evidence shows neuronal aggregates adjacent to lesions in sensorimotor areas can progressively take over damaged neurons' functions, modifying interhemispheric differences in somatotopic organization of sensorimotor cortices and accounting for clinical recovery of motor performance and sensorimotor integration. Similarly, fMRI studies show that recovery from hemiplegic strokes is associated with marked reorganization of activation patterns of specific structures. As dynamic patterns of recovery vary, knowledge about patterns of brain connectivity derived from DTI and fMRI could help predict clinical outcome. This combined approach might be the best way to test the degree of plasticity underlying functional recovery. Further advances will enable selection of appropriate neurorehabilitation therapy for individual patients based on the integrity of white matter tracts and their capacity for functional reorganization.

Studying longitudinal effects on functional networks can help us understand network organization. Further studies are needed to investigate imaging information on the extension, location, and functional hierarchy of cortical brain areas. A more thorough understanding of the mechanisms regulating long-term recovery might lead to more efficacious therapeutic and rehabilitative strategies.

9. References

1. Jauch EC, Saver JL, Adams HP Jr, Bruno A, Connors JJ, Demaerschalk BM, Khatri P, McMullan PW Jr, Qureshi AI, Rosenfield K, Scott PA, Summers DR, Wang DZ, Wintermark M, Yonas H; American Heart Association Stroke Council; Council on Cardiovascular Nursing; Council on Peripheral Vascular Disease; Council on Clinical Cardiology. Guidelines for the early management of patients with acute ischemic stroke: a guideline for healthcare professionals from the American Heart Association/American Stroke Association. Stroke. 2013; 44:870-947.

2. Eissa A, Krass I, Bajorek BV. Optimizing the management of acute ischaemic stroke: a review of the utilization of intravenous recombinant tissue plasminogen activator (tPA). J Clin Pharm Ther. 2012; 37:620-629.

3. Alonso de Leciñana M, Egido JA, Casado I, Ribó M, Dávalos A, Masjuan J, Caniego JL, Martínez Vila E, Díez Tejedor E; por el Comité ad hoc del Grupo de Estudio de Enfermedades Cerebrovasculares de la SEN:, Fuentes Secretaría B, Alvarez-Sabin J, Arenillas J, Calleja S, Castellanos M, Castillo J, Díaz-Otero F, López-Fernández JC, Freijo M, Gállego J, García-Pastor A, Gil-Núñez A, Gilo F, Irimia P, Lago A, Maestre J, Martí-Fábregas J, Martínez-Sánchez P, Molina C, Morales A, Nombela F, Purroy F, Rodríguez-Yañez M, Roquer J, Rubio F, Segura T, Serena J, Simal P, Tejada J, Vivancos J. Guidelines for the treatment of acute ischaemic stroke. Neurologia. 2011 6.

4.Kang DW, Kwon JY, Kwon SU, Kim JS. Wake-up or unclear-onset strokes: are they waking up to the world of thrombolysis therapy? Int J Stroke. 2012; 7:311–320.

5. Serena J, Dávalos A, Segura T, Mostacero E, Castillo J. Stroke on awakening: looking for a more rational management. Cerebrovasc Dis. 2003; 16:128-133.

6. Chen PE, Simon JE, Hill MD, Sohn CH, Dickhoff P, Morrish WF, Sevick RJ, Frayne R. Acute ischemic stroke: accuracy of diffusion-weighted MR imaging-effects of b value and cerebrospinal fluid suppression. Radiology. 2006; 238:232-239.

7. Aoki J, Kimura K, Iguchi Y, Shibazaki K, Sakai K, Iwanaga T. FLAIR can estimate the onset time in acute ischemic stroke patients. J Neurol Sci. 2010; 293:39-44.

8. Shang T, Yavagal DR. Application of acute stroke imaging: selecting patients for revascularization therapy. Neurology. 2012; 79:S86-94.

9. Thomalla G, Cheng B, Ebinger M, Hao Q, Tourdias T, Wu O, Kim JS, Breuer L, Singer OC, Warach S, Christensen S, Treszl A, Forkert ND, Galinovic I, Rosenkranz M, Engelhorn T, Köhrmann M, Endres M, Kang DW, Dousset V, Sorensen AG, Liebeskind DS, Fiebach JB, Fiehler J, Gerloff C; STIR and VISTA Imaging Investigators. DWI-FLAIR mismatch for the identification of patients with acute ischaemic stroke within 4.5h of symptom onset (PRE-FLAIR): a multicentre observational study. Lancet Neurol. 2011; 10:978–986.

10. Thomalla G, Rossbach P, Rosenkranz M, Siemonsen S, Krützelmann A, Fiehler J, Gerloff C. Negative fluid-attenuated inversion recovery imaging identifies acute ischemic stroke at 3 hours or less. Ann Neurol. 2009; 65:724-732.

11. Sakai K, Yamada K, Nagakane Y, Mori S, Nakagawa M, Nishimura T. Diffusion tensor imaging may help the determination of time at onset in cerebral ischaemia. J Neurol Neurosurg Psychiatr. 2009; 80:986–990.

12. Mukherjee P, Berman JI, Chung SW, Hess CP, Henry RG. Diffusion tensor MR imaging and fiber tractography: theoretic underpinnings. AJNR Am J Neuroradiol. 2008; 29:632–641.

13. Mukherjee P, Chung SW, Berman JI, Hess CP, Henry RG. Diffusion tensor MR imaging and fiber tractography: technical considerations. AJNR Am J Neuroradiol 2008; 29:843–852.

14. Pierpaoli C, Barnett A, Pajevic S, Chen R, Penix LR, Virta A, Basser P. Water diffusion changes in wallerian degeneration and their dependence on white matter architecture. Neuroimage 2001; 13:1174–1185.

15. Virta A, Barnett A, Pierpaoli C. Visualizing and characterizing white matter fiber structure and architecture in the human corticospinal tract using diffusion tensor MRI. Magn Reson Imaging 1999; 17:1121–1133.

16. Shereen A, Nemkul N, Yang D, Adhami F, Dunn RS, Hazen ML, Nakafuku M, Ning G, Lindquist DM, Kuan CY. Ex vivo diffusion tensor imaging and neuropathological correlation in a murine model of hypoxia-ischemia-induced thrombotic stroke. J Cereb Blood Flow Metab. 2011; 31:1155–1169.

17. Bhagat YA, Hussain MS, Stobbe RW, Butcher KS, Emery DJ, Shuaib A, Siddiqui MM, Maheshwari P, Al-Hussain F, Beaulieu C. Elevations of diffusion anisotropy are associated with hyper-acute stroke: a serial imaging study. Magn Reson Imaging. 2008; 26:683–693.

18. Liu Y, D'Arceuil HE, Westmoreland S, He J, Duggan M, Gonzalez RG, Pryor J, de Crespigny AJ. Serial diffusion tensor MRI after transient and permanent cerebral ischemia in nonhuman primates. Stroke. 2007; 38:138–145.

19. Bhagat YA, Emery DJ, Shuaib A, Sher F, Rizvi NH, Akhtar N, Clare TL, Leatherdale T, Beaulieu C. The relationship between diffusion anisotropy and time of onset after stroke. J Cereb Blood Flow Metab. 2006; 26:1442–1450.

20. Ozsunar Y, Grant PE, Huisman TA, Schaefer PW, Wu O, Sorensen AG, Koroshetz WJ, Gonzalez RG. Evolution of water diffusion and anisotropy in hyperacute stroke: significant correlation between fractional anisotropy and T2. AJNR Am J Neuroradiol. 2004; 25:699–705.

21. Yang Q, Tress BM, Barber PA, Desmond PM, Darby DG, Gerraty RP, Li T, Davis SM. Serial study of apparent diffusion coefficient and anisotropy in patients with acute stroke. Stroke. 1999; 30:2382–2390.

22. Duncan PW, Goldstein LB, Matchar D, Divine GW, Feussner J. Measurement of motor recovery after stroke: outcome assessment and sample size requirements. Stroke 1992;23:1084–1089.

23. Coupar F, Pollock A, Rowe P, Weir C, Langhorne P. Predictors of upper limb recovery after stroke: a systematic review and meta-analysis. Clin Rehabil. 2012; 26:291–313.

24. Hendricks HT, van Limbeek J, Geurts AC, Zwarts MJ. Motor recovery after stroke: a systematic review of the literature. Arch Phys Med Rehabil 2002; 83:1629–1637.

25. Prabhakaran S, Zarahn E, Riley C, Speizer A, Chong JY, Lazar RM, Marshall RS, Krakauer JW. Inter-individual variability in the capacity for motor recovery after ischemic stroke. Neurorehabil Neural Repair 2008; 22:64–71.

26. Schiemanck SK, Kwakkel G, Post MW, Kappelle LJ, Prevo AJ. Impact of internal capsule lesions on outcome of motor hand function at one year post-stroke. J Rehabil Med 2008; 40:96–101.

27. Nelles M, Gieseke J, Flacke S, et al. Diffusion tensor pyramidal tractography in patients with anterior choroidal artery infarcts. AJNR Am J Neuroradiol 2008; 29:488–493.

28. Lai C, Zhang SZ, Liu HM, et al. White matter tractography by diffusion tensor imaging plays an important role in prognosis estimation of acute lacunar infarctions. Br J Radiol 2007; 80:782– 789.

29. Jang SH, Bai D, Son SM, et al. Motor outcome prediction using diffusion tensor tractography in pontine infarct. Ann Neurol 2008; 64:460–465.

30. Cho SH, Kim DG, Kim DS, et al. Motor outcome according to the integrity of the corticospinal tract determined by diffusion tensor tractography in the early stage of corona radiata infarct. Neurosci Lett 2007; 426:123–127.

31. Konishi J, Yamada K, Kizu O, et al. MR tractography for the evaluation of functional recovery from lenticulostriate infarcts. Neurology 2005; 64:108–113.

32. Lee JS, Han MK, Kim SH, et al. Fiber tracking by diffusion tensor imaging in corticospinal tract stroke: Topographical correlation with clinical symptoms. Neuroimage 2005; 26:771–76

33. Thomalla G, Glauche V, Weiller C, et al. Time course of Wallerian degeneration after ischaemic stroke revealed by diffusion tensor imaging. J Neurol Neurosurg Psychiatry 2005; 76:266–68

34. Puig J, Pedraza S, Blasco G, Daunis-I-Estadella J, Prados F, Remollo S, Prats-Galino A, Soria G, Boada I, Castellanos M, Serena J. Wallerian degeneration in the corticospinal tract evaluated by diffusion tensor imaging correlates with motor deficit 30 days after middle cerebral artery ischemic stroke. AJNR Am J Neuroradiol 2010; 31:1324-1330.

35. Nucifora PG, Verma R, Lee SK, et al. Diffusion-tensor MR imaging and tractography: exploring brain microstructure and connectivity. Radiology 2007; 245:367-384

36. Chung HW, Chou MC, Chen CY. Principles and limitations of computational algorithms in clinical diffusion tensor MR tractography. AJNR Am J Neuroradiol 2011; 32:3-13.

37. Møller M, Frandsen J, Andersen G, et al. Dynamic changes in corticospinal tracts after stroke detected by fibretracking. J Neurol Neurosurg Psychiatry 2007; 78:587–92. 35.

38. Ludeman NA, Berman JI, Wu YW, et al. Diffusion tensor imaging of the corticospinal tracts in infants with motor dysfunction. Neurology 2008; 71: 1676–1682.

39. Liang Z, Zeng J, Zhang C, et al. Longitudinal investigations on the anterograde and retrograde degeneration in the corticospinal tract following pontine infarction with diffusion tensor imaging. Cerebrovasc Dis 2008; 25:209–216.

40. Khong PL, Zhou LJ, Ooi GC, et al. The evaluation of wallerian degeneration in chronic paediatric middle cerebral artery infarction using diffusion tensor MR imaging. Cerebrovasc Dis 2004;18:240–247.

41. Liang Z, Zeng J, Liu S, et al. A prospective study of secondary degeneration following subcortical infarction using diffusion tensor imaging. J Neurol Neurosurg Psychiatry 2007; 78:581–586.

42. Watanabe T, Honda Y, Fujii Y, et al. Three-dimensional anisotropy contrast resonance axonography to predict the prognosis for motor function in patients suffering from stroke. J Neurosurg 2001; 94:955–960.

43. Iizuka H, Sakatani K, Young W. Corticofugal axonal degeneration in rats after middle cerebral artery occlusion. Stroke 1989; 20:1396–402.

44. Lexa FJ, Grossman RI, Rosenquist AC. Dyke Award paper: MR of wallerian degeneration in the feline visual system—characterization by magnetization transfer rate with histopathologic correlation. AJNR Am J Neuroradiol 1994; 15:201–212.

45. Pujol J, Martí-Vilalta JL, Junqué C, et al. Wallerian degeneration of the corticospinal tract in capsular infarction studied by magnetic resonance imaging. Stroke 1990;21:404–409

46. Matsusue E, Sugihara S, Fujii S, et al. Wallerian degeneration of the corticospinal tracts: postmortem MR-pathologic correlations. Acta Radiol 2007; 48:690–694

47. Kuhn MJ, Mikulis DJ, Ayoub DM, et al. Wallerian degeneration after cerebral infarction: evaluation with sequential MR imaging. Radiology 1989; 172: 179–182.

48. Puig J, Pedraza S, Blasco G, Daunis-I-Estadella J, Prados F, Remollo S, Prats-Galino A, Soria G, Boada I, Castellanos M, Serena J. Acute damage to the posterior limb of the internal capsule on diffusion tensor tractography as an early imaging predictor of motor outcome after stroke. AJNR Am J Neuroradiol. 2011; 32:857-863.

49. D. Le Bihan. Looking into the functional architecture of the brain with diffusion MRI. Nature Reviews Neuroscience, 4(6):469–480, 2003.

50. E. O. Stejskal and J. E. Tanner. Spin diffusion measurements: spin echoes in the

presence of a time-dependent field gradient. The Journal of Chemical Physics,

42:288–292, 1965.

51. Roberts TP, Schwartz ES. Principles and implementation of diffusion-weighted and diffusion tensor imaging. Pediatr Radiol. 2007;37:739-48.

52. Özarslan E, T. H. Mareci. Generalized diffusion tensor imaging and analytical relationships between diffusion tensor imaging and high angular resolution imaging. Magnetic Resonance in Medicine, 50:955–965, 2003.

53. Basser PJ, Pierpaoli C. Microstructural and physiological features of tissues elucidated by quantitative-diffusion-tensor MRI. Journal of magnetic resonance Series B, 111:209–219, 1996.

54. Basser PJ. Inferring microstructural features and the physiological state of tissues from diffusion-weighted images. NMR in Biomedicine, 8 (7):333–344, 1995.

55. Basser PJ, Pajevic S, Pierpaoli C, Duda J, Aldroubi A. In vivo fiber tractography using DT-MRI data. Magnetic Resonance in Medicine, 44:625– 632, 2000.

56. Mori S, Zijl PC. Fiber tracking: principles and strategies - a technical review. NMR in Biomedicine, 15(7-8):468–480, 2002.

57. Conturo TE, Lori NF, Cull TS, Akbudak E, Snyder AZ, Shimony JS, Mckinstry RC, Burton H, Raichle ME. Tracking neuronal fiber pathways in the living human brain. Magnetic Resonance in Medicine, 35:399–412, 1999.

58. McGraw T, Vemuri BC, Chen Y, Rao M, Mareci TH. DT-MRI denoising and neuronal fiber tracking. Medical image analysis, 8(2):95–111, June 2004.

59. Hagmann P, Thiran JP, Jonasson L, Vandergheynst P, Clarke S, Maeder P, Meuli R. DTI mapping of human brain connectivity: statistical fibre tracking and virtual dissection. NeuroImage. 2003 19:545–554.

60. Behrens TE, Berg HJ, Jbabdi S, Rushworth MF, Woolrich MW. Probabilistic diffusion tractography with multiple fibre orientations: What can we gain? Neuroimage. 2007 1;34:144-55.

61. Behrens TE, Woolrich MW, Jenkinson M, Johansen-Berg H, Nunes RG, Clare S, Matthews PM, Brady JM, Smith SM. Characterization and propagation of uncertainty in diffusion-weighted MR imaging. Magn Reson Med. 2003;50:1077-88.

62. Koch MA, Norris DG, Hund-Georgiadis M. An investigation of functional and anatomical connectivity using magnetic resonance imaging. Neuroimage. 2002;16:241-50.

63. Jbabdi S, Bellec P, Toro R, Daunizeau J, Pélégrini-Issac M, Benali H. Accurate anisotropic fast marching for diffusion-based geodesic tractography. Int J Biomed Imaging. 2008;2008:320195.

64. X. Wu, Q. Xu, L. Xu, J. Zhou, A. W. Anderson, and Z. Ding. Genetic white matter

fiber tractography with global optimization. Journal of neuroscience methods. 2009 184:375–9.

65. Rosenberg GA. Ischemic brain edema. Prog Cardiovasc Dis. 1999; 42:209-216.

66. Cho AH, Sohn SI, Han MK, et al. Safety and efficacy of MRI-based thrombolysis in unclear-onset stroke: a preliminary report. Cerebrovasc Dis 2008; 25: 572–579.

67. Moseley ME, Kucharczyk J, Mintorovitch J, et al. Diff usion-weighted MR imaging of acute stroke: correlation with T2-weighted and magnetic susceptibility-enhanced MR imaging in cats. AJNR Am J Neuroradiol 1990; 11: 423–429.

68. Hoehn-Berlage M, Eis M, Back T, Kohno K, Yamashita K. Changes of relaxation times (T1, T2) and apparent diffusion coefficient after permanent middle cerebral artery occlusion in the rat: temporal evolution, regional extent, and comparison with histology. Magn Reson Med 1995; 34: 824–834.

69. Hajnal JV, Bryant DJ, Kasuboski L, et al. Use of fluid attenuated inversion recovery (FLAIR) pulse sequences in MRI of the brain. J Comput Assist Tomogr 1992; 16: 841–844.

70. Carano RA, Li F, Irie K, Helmer KG, Silva MD, Fisher M, Sotak CH. Multispectral analysis of the temporal evolution of cerebral ischemia in the rat brain. J Magn Reson Imaging. 2000;12:842-858.

71. Muñoz Maniega S, Bastin ME, Armitage PA, Farrall AJ, Carpenter TK, Hand PJ, Cvoro V, Rivers CS, Wardlaw JM. Temporal evolution of water diffusion parameters is different in grey and white matter in human ischaemic stroke. J Neurol Neurosurg Psychiatry. 2004;75:1714-1718.

72. Pajevic S, Pierpaoli C. Color schemes to represent the orientation of anisotropic tissues from diffusion tensor data: application to white matter fiber tract mapping in the human brain. Magn Reson Med 1999;42:526–40.

73. Liang Z, Zeng J, Liu S, et al. A prospective study of secondary degeneration following subcortical infarction using diffusion tensor imaging. J Neurol Neurosurg Psychiatry 2007;78:581–86.

74. Watanabe T, Honda Y, Fujii Y, et al. Three-dimensional anisotropy contrast resonance axonography to predict the prognosis for motor function in patients suffering from stroke. J Neurosurg 2001;94:955–60.

75. Mukherjee P, Chung SW, Berman JI, et al. Diffusion tensor MR imaging and fiber tractography: technical considerations. AJNR Am J Neuroradiol 2008;29:843–52

76. Lazar M, Weinstein DM, Tsuruda KM, et al. White matter tractography using diffusion tensor deflection. Hum Brain Mapp 2003;18:306–21.

77. Wakana S, Jiang H, Nagae-Poetscher LM, et al. Fiber tract-based atlas of human white matter anatomy. Radiology 2004;230:77–87

78. Sorensen AG, Wu O, Copen WA, Davis TL, Gonzalez RG, Koroshetz WJ, Reese TG, Rosen BR, Wedeen VJ, Weisskoff RM. Human acute cerebral ischemia: detection of changes in water diffusion anisotropy by using MR imaging. Radiology. 1999;212:785-792.

79. Morita N, Harada M, Uno M, Furutani K, Nishitani H. Change of diffusion anisotropy in patients with acute cerebral infarction using statistical parametric analysis. Radiat Med. 2006;24:253-259.

80. Harris AD, Pereira RS, Mitchell JR, Hill MD, Sevick RJ, Frayne R. A comparison of images generated from diffusion-weighted and diffusion-tensor imaging data in hyper-acute stroke. J Magn Reson Imaging. 2004;20:193-200.

81. Davidoff RA. The corticospinal tract. Neurology 1990;40:332–339.

82. Lindberg PG, Skejø PH, Rounis E, Nagy Z, Schmitz C, Wernegren H, Bring A, Engardt M, Forssberg H, Borg J. Wallerian degeneration of the corticofugal tracts in chronic stroke: a pilot study relating diffusion tensor imaging, transcranial magnetic stimulation, and hand function. Neurorehabil Neural Repair 2007 21:551– 560.

83. Kang DW, Chu K, Yoon BW, Song IC, Chang KH, Roh JK. Diffusion-weighted imaging in wallerian degeneration. J Neurol Sci 2000;15;178:167–169.

84. Sawlani V, Gupta RK, Singh MK, Kohli A. MRI demonstration of wallerian degeneration in various intracranial lesions and its clinical implications. J Neurol Sci 1997; 146:103– 108.

85. Orita T, Tsurutani T, Izumihara A, Kajiwara K, Matsunaga T. Corticospinal tract wallerian degeneration and correlated symptoms in stroke. Eur J Radiol 1994; 18:26–29.

86. Castillo M, Mukherji SK. Early abnormalities related to postinfarction wallerian degeneration: evaluation withMRdiffusion-weighted imaging. J Comput Assist Tomogr 1999; 23:1004–1007.

87. Thomalla G, Glauche V, Koch MA, Beaulieu C, Weiller C, Röther J. Diffusion tensor imaging detects early wallerian degeneration of the pyramidal tract after ischemic stroke. Neuroimage 2004; 22:1767–1774.

88. Werring DJ, Toosy AT, Clark CA, Parker GJ, Barker GJ, Miller DH, Thompson AJ. Diffusion tensor imaging can detect and quantify corticospinal tract degeneration after stroke. J Neurol Neurosurg Psychiatry 2000; 69:269–272.

89. Møller M, Frandsen J, Andersen G, Gjedde A, Vestergaard-Poulsen P, Østergaard L. Dynamic changes in corticospinal tracts after stroke detected by fibretracking. J Neurol Neurosurg Psychiatry 2007;78:587–592.

90. Crocker T, Forster A, Young J, Brown L, Ozer S, Smith J, Green J, Hardy J, Burns E, Glidewell E, Greenwood DC. Physical rehabilitation for older people in long-term care. Cochrane Database Syst Rev. 2013 Feb 28;2:CD004294. doi: 10.1002/14651858.

91. Li L, Jiang Q, Ding G, Zhang L, Zhang ZG, Li Q, Panda S, Kapke A, Lu M, Ewing JR, Chopp M. MRI identification of white matter reorganization enhanced by erythropoietin treatment in a rat model of focal ischemia. Stroke 2009; 40:936–941.

92. Bang OY, Lee JS, Lee PH, Lee G. Autologous mesenchymal stem cell transplantation in stroke patients. Ann Neurol 2005; 57:874–882.

93. Sulter G, Steen C, De Keyser J. Use of the Barthel index and modified Rankin scale in acute stroke trials.Stroke 1999;30:1538-41.

94. The HBP Report. The Human Brain Project. April 2012.

95. Craddock RC, Jbabdi S, Yan CG, Vogelstein JT, Castellanos FX, Di Martino A, Kelly C, Heberlein K, Colcombe S, Milham MP. Imaging human connectomes at the macroscale. Nat Methods. 2013 Jun;10(6):524-39.

96. Song M, Jiang T. A review of functional magnetic resonance imaging for Brainnetome. Neurosci Bull. 2012 Aug;28(4):389-98.

10. Annexes

10.1.   National Institute of Health Stroke Scale (NIHSS)

Instructions	Scale Definition	Score
1a. Level of Consciousness: The investigator must choose a response if a full evaluation is prevented by such obstacles as an endotracheal tube, language barrier, orotracheal trauma/bandages. A 3 is scored only if the patient makes no movement (other than reflexive posturing) in response to noxious stimulation.	0 = Alert; keenly responsive. 1 = Not alert; but arousable by minor stimulation to obey, answer, or respond. 2 = Not alert; requires repeated stimulation to attend, or is obtunded and requires strong or painful stimulation to make movements (not stereotyped). 3 = Responds only with reflex motor or autonomic effects or totally unresponsive, flaccid, and areflexic.	———
1b. LOC Questions: The patient is asked the month and his/her age. The answer must be correct - there is no partial credit for being close. Aphasic and stuporous patients who do not comprehend the questions will score 2. Patients unable to speak because of endotracheal intubation, orotracheal trauma, severe dysarthria from any cause, language barrier, or any other problem not secondary to aphasia are given a 1. It is important that only the initial answer be graded and that the examiner not "help" the patient with verbal or non-verbal cues.	0 = Answers both questions correctly. 1 = Answers one question correctly. 2 = Answers neither question correctly.	———
1c. LOC Commands: The patient is asked to open and close the eyes and then to grip and release the non-paretic hand. Substitute another one step command if the hands cannot be used. Credit is given if an unequivocal attempt is made but not completed due to weakness. If the patient does not respond to command, the task should be demonstrated to him or her (pantomime), and the result scored (i.e., follows none, one or two commands). Patients with trauma, amputation, or other physical impediments should be given suitable one-step commands. Only the first attempt is scored.	0 = Performs both tasks correctly. 1 = Performs one task correctly. 2 = Performs neither task correctly.	———
2. Best Gaze: Only horizontal eye movements will be tested. Voluntary or reflexive (oculocephalic) eye movements will be scored, but caloric testing is not done. If the patient has a conjugate deviation of the eyes that can be overcome by voluntary or reflexive activity, the score will be 1. If a patient has an isolated peripheral nerve paresis (CN III, IV or VI), score a 1. Gaze is testable in all aphasic patients. Patients with ocular trauma, bandages, pre-existing blindness, or other disorder of visual acuity or fields should be tested with reflexive movements, and a choice made by the investigator. Establishing eye contact and then moving about the patient from side to side will occasionally clarify the presence of a partial gaze palsy.	0 = Normal. 1 = Partial gaze palsy; gaze is abnormal in one or both eyes, but forced deviation or total gaze paresis is not present. 2 = Forced deviation, or total gaze paresis not overcome by the oculocephalic maneuver.	———
3. Visual: Visual fields (upper and lower quadrants) are tested by confrontation, using finger counting or visual threat, as appropriate. Patients may be encouraged, but if they look at the side of the moving fingers appropriately, this can be scored as normal. If there is unilateral blindness or enucleation, visual fields in the remaining eye are scored. Score 1 only if a clear-cut asymmetry, including quadrantanopia, is found. If patient is blind from any cause, score 3. Double simultaneous stimulation is performed at this point. If there is extinction, patient receives a 1, and the results are used to respond to item 11.	0 = No visual loss. 1 = Partial hemianopia. 2 = Complete hemianopia. 3 = Bilateral hemianopia (blind including cortical blindness).	———

4. Facial Palsy: Ask – or use pantomime to encourage – the patient to show teeth or raise eyebrows and close eyes. Score symmetry of grimace in response to noxious stimuli in the poorly responsive or non-comprehending patient. If facial trauma/bandages, orotracheal tube, tape or other physical barriers obscure the face, these should be removed to the extent possible.

0 = Normal symmetrical movements.

1 = Minor paralysis (flattened nasolabial fold, asymmetry on smiling).

2 = Partial paralysis (total or near-total paralysis of lower face).

3 = Complete paralysis of one or both sides (absence of facial movement in the upper and lower face).

———

5. Motor Arm: The limb is placed in the appropriate position: extend the arms (palms down) 90 degrees (if sitting) or 45 degrees (if supine). Drift is scored if the arm falls before 10 seconds. The aphasic patient is encouraged using urgency in the voice and pantomime, but not noxious stimulation. Each limb is tested in turn, beginning with the non-paretic arm. Only in the case of amputation or joint fusion at the shoulder, the examiner should record the score as untestable (UN), and clearly write the explanation for this choice.

0 = No drift; limb holds 90 (or 45) degrees for full 10 seconds.

1 = Drift; limb holds 90 (or 45) degrees, but drifts down before full 10 seconds; does not hit bed or other support.

2 = Some effort against gravity; limb cannot get to or maintain (if cued) 90 (or 45) degrees, drifts down to bed, but has some effort against gravity.

3 = No effort against gravity; limb falls.

4 = No movement.

UN = Amputation or joint fusion, explain:
_____

5a. Left Arm

5b. Right Arm

———
———

6. Motor Leg: The limb is placed in the appropriate position: hold the leg at 30 degrees (always tested supine). Drift is scored if the leg falls before 5 seconds. The aphasic patient is encouraged using urgency in the voice and pantomime, but not noxious stimulation. Each limb is tested in turn, beginning with the non-paretic leg. Only in the case of amputation or joint fusion at the hip, the examiner should record the score as untestable (UN), and clearly write the explanation for this choice.

0 = No drift; leg holds 30-degree position for full 5 seconds.

1 = Drift; leg falls by the end of the 5-second period but does not hit bed.

2 = Some effort against gravity; leg falls to bed by 5 seconds, but has some effort against gravity.

3 = No effort against gravity; leg falls to bed immediately.

4 = No movement.

UN = Amputation or joint fusion, explain: _____

6a. Left Leg

6b. Right Leg

———

7. Limb Ataxia: This item is aimed at finding evidence of a unilateral cerebellar lesion. Test with eyes open. In case of visual defect, ensure testing is done in intact visual field. The finger-nose-finger and heel-shin tests are performed on both sides, and ataxia is scored only if present out of proportion to weakness. Ataxia is absent in the patient who cannot understand or is paralyzed. Only in the case of amputation or joint fusion, the examiner should record the score as untestable (UN), and clearly write the explanation for this choice. In case of blindness, test by having the patient touch nose from extended arm position.

0 = Absent.

1 = Present in one limb.

2 = Present in two limbs.

UN = Amputation or joint fusion, explain: _____

_____

8. Sensory: Sensation or grimace to pinprick when tested, or withdrawal from noxious stimulus in the obtunded or aphasic patient. Only sensory loss attributed to stroke is scored as abnormal and the examiner should test as many body areas (arms [not hands], legs, trunk, face) as needed to accurately check for hemisensory loss. A score of 2, "severe or total sensory loss," should only be given when a severe or total loss of sensation can be clearly demonstrated. Stuporous and aphasic patients will, therefore, probably score 1 or 0. The patient with brainstem stroke who has bilateral loss of sensation is scored 2. If the patient does not respond and is quadriplegic, score 2. Patients in a coma (item 1a=3) are automatically given a 2 on this item.

0 = Normal; no sensory loss.

1 = Mild-to-moderate sensory loss; patient feels pinprick is less sharp or is dull on the affected side; or there is a loss of superficial pain with pinprick, but patient is aware of being touched.

2 = Severe to total sensory loss; patient is not aware of being touched in the face, arm, and leg.

_____

9. Best Language: A great deal of information about comprehension will be obtained during the preceding sections of the examination. For this scale item, the patient is asked to describe what is happening in the attached picture, to name the items on the attached naming sheet and to read from the attached list of sentences. Comprehension is judged from responses here, as well as to all of the commands in the preceding general neurological exam. If visual loss interferes with the tests, ask the patient to identify objects placed in the hand, repeat, and produce speech. The intubated patient should be asked to write. The patient in a coma (item 1a=3) will automatically score 3 on this item. The examiner must choose a score for the patient with stupor or limited cooperation, but a score of 3 should be used only if the patient is mute and follows no one-step commands.

0 = No aphasia; normal.

1 = Mild-to-moderate aphasia; some obvious loss of fluency or facility of comprehension, without significant limitation on ideas expressed or form of expression. Reduction of speech and/or comprehension, however, makes conversation about provided materials difficult or impossible. For example, in conversation about provided materials, examiner can identify picture or naming card content from patient's response.

2 = Severe aphasia; all communication is through fragmentary expression; great need for inference, questioning, and guessing by the listener. Range of information that can be exchanged is limited; listener carries burden of communication. Examiner cannot identify materials provided from patient response.

3 = Mute, global aphasia; no usable speech or auditory comprehension.

_____

10. Dysarthria: If patient is thought to be normal, an adequate sample of speech must be obtained by asking patient to read or repeat words from the attached list. If the patient has severe aphasia, the clarity of articulation of spontaneous speech can be rated. Only if the patient is intubated or has other physical barriers to producing speech, the examiner should record the score as untestable (UN), and clearly write an explanation for this choice. Do not tell the patient why he or she is being tested.

0 = Normal.

1 = Mild-to-moderate dysarthria; patient slurs at least some words and, at worst, can be understood with some difficulty.

2 = Severe dysarthria; patient's speech is so slurred as to be unintelligible in the absence of or out of proportion to any dysphasia, or is mute/anarthric.

UN = Intubated or other physical barrier, explain:_____

_____

11. Extinction and Inattention (formerly Neglect): Sufficient information to identify neglect may be obtained during the prior testing. If the patient has a severe visual loss preventing visual double simultaneous stimulation, and the cutaneous stimuli are normal, the score is normal. If the patient has aphasia but does appear to attend to both sides, the score is normal. The presence of visual spatial neglect or anosagnosia may also be taken as evidence of abnormality. Since the abnormality is scored only if present, the item is never untestable.

0 = No abnormality.

1 = Visual, tactile, auditory, spatial, or personal inattention or extinction to bilateral simultaneous stimulation in one of the sensory modalities.

2 = Profound hemi-inattention or extinction to more than one modality; does not recognize own hand or orients to only one side of space.

10.2. Modified Rankin Scale (MRS)

Score Description

0   No symptoms at all

1   No significant disability despite symptoms; able to carry out all usual duties and activities

2   Slight disability; unable to carry out all previous activities, but able to look after own affairs without assistance

3   Moderate disability; requiring some help, but able to walk without assistance

4   Moderately severe disability; unable to walk without assistance and unable to attend to own bodily needs without assistance

5   Severe disability; bedridden, incontinent and requiring constant nursing care and attention

6   Dead

TOTAL (0–6):

10.3.   Barthel Index (BI)

Activity Score

FEEDING
0 = unable
5 = needs help cutting, spreading butter, etc., or requires modified diet
10 = independent

_____

BATHING
0 = dependent
5 = independent (or in shower)

_____

GROOMING
0 = needs to help with personal care
5 = independent face/hair/teeth/shaving (implements provided)

_____

DRESSING
0 = dependent
5 = needs help but can do about half unaided
10 = independent (including buttons, zips, laces, etc.)

_____

BOWELS
0 = incontinent (or needs to be given enemas)
5 = occasional accident
10 = continent

_____

BLADDER
0 = incontinent, or catheterized and unable to manage alone
5 = occasional accident
10 = continent

_____

TOILET USE
0 = dependent
5 = needs some help, but can do something alone
10 = independent (on and off, dressing, wiping)

_____

TRANSFERS (BED TO CHAIR AND BACK)
0 = unable, no sitting balance
5 = major help (one or two people, physical), can sit
10 = minor help (verbal or physical)
15 = independent

_____

MOBILITY (ON LEVEL SURFACES)
0 = immobile or < 50 yards
5 = wheelchair independent, including corners, > 50 yards
10 = walks with help of one person (verbal or physical) > 50 yards
15 = independent (but may use any aid; for example, stick) > 50 yards

_____

STAIRS
0 = unable
5 = needs help (verbal, physical, carrying aid)
10 = independent

_____

TOTAL (0–100):   _____

10.4.   Motricity Index

ARM   TO BE CONDUCTED IN SITTING POSITION

1. Pinch grip   (*2.5cm cube between thumb and forefinger).*

2. Elbow flexion   (*from 90 , voluntary contraction/movement*)

3. Shoulder abduction   (*from against chest*)

LEG   TO BE CONDUCTED IN SITTING POSITION

4. Ankle dorsiflexion   (*from plantar flexed position*)

5. Knee extension   (*from 90 ,o voluntary contraction/movement*)

6. Hip flexion   (*usually from 90º*)

TEST 1 (Pinch grip)
0 = No movement
11 = Beginnings of prehension
19 = Grips cube but unable to hold against gravity.
22 = Grips cube, held against gravity but not against weak pull.
26 = Grips cube against pull but weaker than other/normal side.
33 = Normal pinch grip

TESTS 2 - 6
0 = No movement
9 = Palpable contraction in muscle but no movement.
14 = Movement seen but not full range/not against gravity.
19 = Full range against gravity, not against resistance.
25 = Movement against resistance but weaker than other side.
33 = Normal power

ARM SCORE (1+2+3)

LEG SCORE (4+5+6)

SIDE SCORE (Arm + leg)/2